Summer 7-26-2018

Effects of drift macroalgae on sediment nitrogen cycling in Thalassia testudinum beds of St. Joseph Bay, FL

Erica Strope

Title: Effects of drift macroalgae on sediment nitrogen cycling in *Thalassia testudinum* beds of St. Joseph Bay, FL

Erica K. Strope
Master's in Integrative Biology Program, 2018
Kennesaw State University

Committee Members: Dr. Troy Mutchler, Dr. Mark J. McCarthy, Dr. Joseph Dirnberger, Dr. Daniel Ferreira

Abstract

Anthropogenic nitrogen (N) loading and eutrophication can affect valuable ecosystem services and seagrass habitats by modifying structural and functional aspects of estuarine communities including increasing and prolonging macroalgae blooms. In some contexts, macroalgae may play a key role in N cycling pathways because they can alter sediment chemistry. Previous research has associated drift macroalgae blooms with elevated dissolved inorganic N concentrations in sediments as a result of increased remineralization of organic matter, but drift macroalgae effects on microbial N transformation pathways are not well understood. This study quantified the effects of macroalgae on estuarine N cycling in *Thalassia testudinum* seagrass beds of St. Joseph Bay, FL, on June 4, 18, and 26, 2017. Sediment physical characteristics, seagrass and macroalgae biomass measurements, and porewater chemistry were analyzed to compare sediments in areas with and without macroalgae cover. Seagrass aboveground and belowground biomass was significantly greater in areas with no macroalgae on June 18, and 26. Sediments at incubation sites with macroalgae had higher porewater sulfide and % organic matter, though this was not significant across all sites and incubation dates. Porewater sulfide concentrations were positively correlated to seagrass shoot density in areas with and without drift macroalgae. A continuous-flow incubation system for intact sediment cores amended with stable isotope additions ($^{15}NH_4^+$ and $^{15}NO_3^-$) was used to measure N transformation rates across the sediment-water interface. Results shows that DNRA (dissimilatory nitrate reduction to ammonium) rates were similar in magnitude to denitrification rates in areas with and without macroalgae, showing

similar rates of N removal and recycling within sediments. Anammox rates were a minor source of N_2 flux from sediments in macroalgae and no macroalgae areas, though anammox was stimulated under drift macroalgae blooms. N fixation was observed during all incubations, even in sediments with porewater NH_4^+ above 300 µM. Previous research in St. Joseph Bay during summer and fall had higher denitrification rates, and lower N fixation rates than this study. Presence of drift macroalgae appears to possibly alter organic matter supply during blooms that may affect seasonal sediment N cycling rates in seagrass beds. Though there were not many significant differences in N cycling rates between areas with and without drift macroalgae, data presented in this study provides baseline N transformation rates in a relatively unimpacted bay, St. Joseph Bay, FL, and is an important step in understanding how nutrient loading may alter N cycling rates in other similar systems.

Introduction

In coastal marine ecosystems, understanding nitrogen (N) cycling is increasingly important due to the growing problem of excessive nutrient loading (Joye and Anderson 2008), primarily in the form of fertilizer runoff, atmospheric deposition (natural and anthropogenic sources), and wastewater inputs (e.g., Galloway et al. 2003). Increased nutrient (N and phosphorus (P)) concentrations have been associated with eutrophication in aquatic systems (McCarthy et al. 2016) often increasing primary production (Beman et al. 2005) and harmful algal blooms (Heisler et al. 2008), decreasing water column oxygen concentrations (Beman et al. 2005; Boesch et al. 2009), and changing food web dynamics (Vitousek et al. 1997). N cycling pathways govern the fate of N within ecosystems, so to understand the effects of eutrophication, we must understand N cycling in natural and modified systems.

Different pathways of the N cycle occur under oxic and suboxic conditions (Figure 1), a transition that usually occurs near the sediment-water interface, within a few millimeters of the sediment surface (Santschi et al. 1990). N cycling rates are also affected by other environmental and temporal factors including salinity, temperature, availability of carbon, and sulfide concentrations (e.g. An and Gardner 2002; Gardner et al. 2006) These factors, among others, influence what pathways are favored in different ecosystems (Gardner et al. 2006; Burgin and Hamilton 2007; Joye and Anderson 2008). Anaerobic N transformations include denitrification, dissimilatory nitrate reduction to NH_4^+ (DNRA), remineralization of organic matter (OM), and

anammox (anaerobic NH_4^+ oxidation). Denitrification reduces nitrate (NO_3^-) to nitrite (NO_2^-), then to nitric oxide (NO), nitrous oxide (N_2O), and N_2 gas (Payne 1973). DNRA transforms NO_3^- to NH_4^+ via NO_2^- (Tiedje 1988), anammox uses NO_2^- to oxidize NH_4^+ to N_2 gas (Mulder et al. 1995), and remineralization breaks down OM to simpler compounds, such as organic carbon and NH_4^+. Denitrification and anammox export N from ecosystems as N_2 gas, while DNRA and remineralization promote recycling of bioavailable N in the form of NH_4^+ (Capone and Carpenter 1982; Burgin and Hamilton 2007). Aerobic pathways that occur in the top few millimeters of sediments are nitrification and OM remineralization (occurs in both aerobic and anaerobic). N fixation is the process of transforming N_2 gas into more readily useable NH_4^+, which can be assimilated into biomass (Capone and Carpenter 1982), while nitrification oxidizes NH_4^+ to NO_2^- then NO_3^- (Ward 2008). The rates of these transformations can determine the net balance of available N forms in an ecosystem, which can ultimately influence the productivity of the system and possibly exacerbate effects of eutrophication (e.g., McCarthy et al. 2016).

Rates of N pathways have been measured in many coastal environments (e.g., Eyre et al. 2013; Smyth et al. 2013), including seagrass ecosystems (e.g., McGlathery et al. 1998; Eyre et al. 2013; Salk et al. 2017), but no known studies have determined sediment-water interface N transformation rates in seagrass systems under drift macroalgae blooms. N transformation rates, and what drives these processes, are still not well understood in seagrasses because there are so few estimates, and these rates can vary regionally and seasonally (e.g. Eyre et al. 2011; Eyre et al 2013; Salk et al. 2017).

Seagrasses, marine angiosperms, are important ecosystem engineers that can modify water flow and sediment grain size and provide habitat for many different species of vertebrates and invertebrates, including commercially and recreationally important species (Hemminga and Duarte 2000; Beck et al. 2001). Seagrass communities also sequester, or fix, a significant amount of dissolved carbon dioxide through photosynthesis (Duarte et al. 2005), stabilize coastal sediments against erosion (Orth et al. 2006), and play important roles in biogeochemical cycling in coastal systems (Hemminga and Duarte 2000; McGlathery et al. 2007). Seagrasses are also vulnerable to anthropogenic stressors, and are sensitive to changes in light availability, due to their high photosynthetic needs (Orth et al. 2006). Decreases in light availability are often associated with algae growth, including drift macroalgae, and can therefore influence eutrophication effects in indirect ways (Orth et al. 2006).

Drift macroalgae have garnered more interest in N cycling research due to the increase of anthropogenic N loading to coastal regions causing more persistent and prolonged blooms (Pihl et al. 1995; Osterling and Pihl 2001; Arroyo and Bonsdorff 2016). Drift macroalgae thrives in areas with increased nutrients (e.g., Pedersen et al. 2010), especially NH_4^+ from anthropogenic sources (e.g., Wang et al. 2012) and N flux from sediments (Arroyo and Bonsdorff 2016). Most research, however, has not focused on direct N cycling rate measurements under macroalgae blooms; instead, these studies have only hypothesized how N transformations may be altered due to how macroalgae may affect environmental conditions such as sulfide concentrations, or how the macroalgae assimilates or exudes nutrients into the surrounding water column and sediments (Garcia-Robledo and Corzo 2011; McGlathery et al. 2013).

Drift macroalgae are ephemeral, bloom-forming algae that grow in mats or clumps in the water column, attached to marine vegetation, or on the sediment surface (Arroyo and Bonsdorff 2016). Macroalgae can increase biodiversity in marine systems by providing habitat for a variety of marine organisms (Coastal and Estuarine Studies 2005), but their presence can also be harmful by shading seagrasses and microphytobenthic communities, inhibiting photosynthesis (Hauxwell et al. 2003; Coastal and Estuarine Studies 2005; Garcia-Robledo and Corzo 2011). The effects that drift macroalgae have on seagrasses mostly depends on the residence time of macroalgae in the seagrass beds, if the macroalgae species grows attached to seagrass blades or benthic substrate, and the species of macroalgae and seagrass (Arroyo and Bonsdorff 2016). Water flow velocity and hydrologic conditions often determine how long drift macroalgae remain in an area, while spatial distribution of macroalgae is closely related to seagrass bed morphology (Bell and Hall 1997; Arroyo and Bonsdorff 2016). Distribution of drift macroalgae within seagrass beds is often patchy with a high amount of variability, though drift macroalgae tend to accumulate in small bare patches within the seagrass beds (Arroyo and Bondsdorff 2016). Drift macroalgae mats can move up to 0.5 km per day, but if water velocity is not sufficient to flush-out large macroalgae mats out of the system, then these accumulations will remain in the same areas until they eventually degrade (Holmquist 1997; Arroyo and Bonsdorff 2016).

Both seagrasses and drift macroalgae can impact sediment N transformation rates through a variety of complex, direct and indirect, physical and chemical interactions with their environment. The physical presence of seagrasses reduces water flow velocities (Koch, 1999), that not only promote drift algal accumulation (e.g., Holmquist 1997), but also promotes the

retention of fine sediments (Fonseca and Fisher 1986). Silt-clay percentage of underlying sediments is also positively correlated with the presence of drift macroalgae (Bell and Hall 1997). Sediment size is important because it affects diffusion and advection of nutrients, such as dissolved inorganic N (DIN) and oxygen, across the sediment-water interface, since coarse sediments are more permeable than fine sediments (Asmus et al. 2000; Joye and Anderson 2008). Sediment type can also be important since siliciclastic sediments, which are relatively rich in P and common in northern Florida, can promote N limitation, while carbonate rich sediments promote more P limited environments (Lapointe et al. 1997).

Seagrasses can modify sediment chemistry by oxygenating the rhizosphere during photosynthesis (Frederiksen and Glud 2006), increasing organic matter (OM) content in sediments via detrital inputs, and assimilating and exuding dissolved nutrients, all of which vary seasonally (Eyre et al. 2013). Seagrasses are adapted to live in reduced, anoxic sediments, due to aerenchyma tissue that can protect roots and rhizomes from compounds like sulfide (Homer and Hasler-Sheetal 2014).

The overall effect of macroalgae on sediment chemistry depends on the residence time and bloom stage (i.e., age of drift macroalgae bloom), though there are some common effects (Figure 2). Newly established macroalgae can form mats that assimilate nutrients from the surrounding sediments and water column (Coastal and Estuarine Studies 2005). These mats can act as a barrier between the overlying water column and sediment surface, uncoupling the sediment-water interface and disturbing the flow of dissolved nutrients and gases between the sediment and water column (Coastal and Estuarine Studies 2005). Drift macroalgae cover can also shift the oxic/anoxic boundary from a few millimeters below the sediment surface to the top of the sediments or to the overlying water, primarily due to macroalgae using dissolved oxygen through respiration, and in late stages of blooms, decomposition (Coastal and Estuarine Studies 2005). As macroalgae biomass decomposes, nutrients can be released into the water column and sediment porewaters. This flux of nutrients can then be utilized by opportunistic macro- or microalgae, which can possibly further compound the effects of eutrophication (Garcia-Robledo et al. 2008; Corzo et al. 2009).

Though seagrasses and drift macroalgae are biologically different, they similarly influence, or combine, to alter N transformation pathways and rates by affecting NH4+ pools. NH_4^+ exuded from seagrasses, drift macroalgae, or the remineralization of OM can promote

coupled nitrification-denitrification by supplying substrate for nitrification (McGlathery et al. 2001). Elevated NH_4^+ concentrations accumulated by macroalgae or from detrital seagrass can also be flushed out, which can keep the water column oxygenated through physically removing macroalgae or detritus and bringing in new, oxygenated water (Cebrian et al. 2014).

Remineralization of OM, whether from seagrasses or macroalgae, supplies organic carbon to microbial communities, often shifting them from net autotrophy to heterotrophy, increasing sediment oxygen demand (SOD), and promoting sulfate reduction to sulfide, which can increase H_2S concentrations in sediments (e.g., Hemminga and Duarte, 2000; Corzo et al. 2009; Garcia-Robledo and Corzo 2011). OM remineralization naturally occurs in seagrass sediments, but OM from drift macroalgae can lead to H_2S accumulation in sediment porewaters at concentrations that are toxic to seagrasses (Koch and Erskine 2001) and can inhibit denitrifying bacteria (Burgin and Hamilton 2007).

The last step of denitrification (transforming N_2O to N_2), as well as nitrification, is inhibited by sulfide, which may favor NO_3^- reduction via DNRA (Burgin and Hamilton 2007; Joye and Anderson 2008) or N_2 production via anammox (Eyre et al. 2013). If denitrification is incomplete, NO_2^- may be released, promoting anammox (Eyre et al. 2013). But, NO_2^- release cannot be solely attributed to incomplete denitrification, since incomplete nitrification and DNRA can both release NO_2^-, as well. Both denitrification and DNRA are anaerobic pathways performed by heterotrophic bacteria that rely on organic carbon sources, as well as NO_3^- as their terminal electron acceptor. However, DNRA has been linked to sulfur oxidation and may be promoted in NO_3^--limited sediments with ample labile carbon (Burgin and Hamilton 2007). Relative lability of organic matter is associated with the ratio of carbon (C) to N content in plant tissues. Higher C:N ratios denote that there is more carbon than nitrogen, meaning the tissues are more refractory than low C:N ratios with high N content. Mean C:N (carbon: nitrogen) ratios for *Thalassia testudinum*, on average, is 24.6:1 (Fourqurean and Zieman 2002) while *Laurentia poitei*, a similar species of drift macroalgae from this study, is reported being 10.2:1 (NOAA 1986). Drift macroalgae is more labile than seagrass, and as both degrade, areas with drift macroalgae cover could promote DNRA over denitrification (Eyre et al. 2013; Burgin and Hamilton 2007).

Denitrification has long been thought to be the primary pathway for NO_3^- removal in many coastal ecosystems (Giblin et al. 2013), including seagrasses (Gardner and McCarthy

2009; Eyre et al. 2013), but there is evidence that DNRA rates can be equal to or higher than denitrification in seagrasses (An and Gardner 2002; Aoki et al. 2017; Salk et al. 2017). Additionally, anammox may be an important pathway for N removal as well (e.g., Salk et al. 2017). Previous research studying N cycling under macroalgae blooms has not estimated DNRA, which can have a significant impact on the fate of whether N is removed or recycled in ecosystems (Burgin and Hamilton 2007). Few studies have used stable isotope techniques and direct measurements of nutrient fluxes to determine differences in N transformation rates in seagrass beds with and without drift macroalgae accumulations.

To examine how drift macroalgae mats affect N cycling in coastal marine sediments, this experiment was conducted in June 2017 in St. Joseph Bay, FL, located in the northeastern Gulf of Mexico. Previous research in St. Joseph Bay measured summer N transformation rates in both seagrass beds and adjacent, unvegetated sediments, providing baseline N cycling information in the bay (Hoffman et al., unpublished). In the present study, a continuous-flow incubation system using stable isotope additions (^{15}N) was used to determine N transformation rates and pathways, while various sediment chemistry and biological samples were collected to address the hypotheses that: (1) denitrification rates would be higher than DNRA regardless of macroalgae presence, due to denitrification being more energetically favorable than DNRA; (2) areas with drift macroalgae beds would have higher rates of DNRA than areas without macroalgae due to increased sediment % OM and sulfide concentrations; and (3) N cycling rates will change over the duration of the drift macroalgae bloom; i.e., when the drift macroalgae is in large mats, chemical interactions will be different than during decomposition, possibly altering N transformation rates according to bloom stage.

Methods

Site descriptions

St. Joseph Bay, FL (Figure 3), is located in the northeastern Gulf of Mexico, bounded by Cape San Blas to the west and south and mainland Florida to the east. The bay is 295.4 km^2 in size with no major freshwater inputs (Heck et al. 2000). Salinity ranges from 23-40 (mean = 35), and rainfall averages 1.5 m per year (FDEP 2008). The average water depth is approximately 6.4 m, with maximum depths of 10.7 m towards the northern part of the bay and an average of 0.9 m towards the south (Figure 4-A; FDEP 2008). St. Joseph Bay has diurnal tides with a tidal range

of 0.5 m and temperate climate that is occasionally influenced by subtropical storms and hurricanes during late summer and fall (Stewart, 1962;National Ocean Service, 1988).

The area around St. Joseph Bay is not heavily developed, though increases in nutrient concentrations have been observed since the early 2000's (FDEP 2008). The dominant species of seagrass are *Thalassia testudinum* Banks & Sol. Ex K.D. Koenig, *Halodule wrightii* Ascherson, and *Syringodium filiforme* Kütz, which together comprise about 13% of the bay's total area (Fig. 4-B; FDEP 2008). The bay experiences seasonal macroalgae blooms dominated by rhodophytes, including species from the genera *Laurentia* and *Gracilaria*, Blooms typically start in late spring, but distribution and abundance of these blooms is not well understood. (FDEP 2008).

This study was conducted at six sites (each sampling location was approximately 20 m x 20 m in size) within continuous *T. testudinum* beds on 4, 18, and 27 June, 2017. Three sites were chosen based on the presence (+M) of macroalgal accumulations that completely covered (100% cover) the seagrass canopy over an area of at least one m^2. Three sites were also selected in continuous seagrass beds with no macroalgal cover (-M). One site of each type (+M and –M) was designated for measurement of sediment-water interface N cycling rates. These sites were located within 40 m of one another at the south end of St. Joseph Bay and were chosen because they had similar % cover of seagrasses, water depth, and tidal influence (Table 10). The remaining sites, two with macroalgae blooms (M1, M2), and two without macroalgae blooms (NM1, NM2) were sampled at representative locations to quantify similarities and differences in sediment characteristics and seagrass biomass throughout the bay (Fig. 3).

Sample Collection and analysis

Chemical and Physical Characteristics

Water samples for ambient nutrient concentration analyses (NH_4^+, NO_3^-, NO_2, urea, and ortho-phosphate; OP) were collected at all sites. Water samples were collected using 60 mL, Luer-Lock syringes with pre-rinsed 0.2 µm Nylon syringe filters. At least 10 mL of site water was used to pre-rinse each filter, and 12.5 mL of filtered water was collected into Falcon tubes and stored on ice until they could be frozen at -18° C. Samples were analyzed using standard procedures on a Lachat Quikchem 8500 flow injection analysis system at Wright State University (WSU).

Triplicate bulk sediment samples were randomly collected to measure sediment grain size, % OM, porewater NH_4^+ and sulfide concentrations, exchangeable NH_4^+, and carbon to nitrogen (C:N) content of sediments. Sediment samples for porewater and exchangeable NH_4^+, sediment grain size, % OM, and C:N analysis were collected using 60 mL syringe corers, extruded into plastic Whirl-Pak bags (Nasco), and chilled on ice until they could be frozen at approximately -18° C until analysis. Porewater was extracted from sediments via centrifugation. For exchangeable NH_4^+, 30 mL of 0.2 M acidified potassium chloride (pH = 2.5) was added to five grams of sediment. The mixture was rotated using a hematology mixer for 20 minutes to extract any NH_4^+ bound to the cation exchange complex (Hatton and Pickering 1990), and NH_4^+ was measured using the phenol hypochlorite method (Solarzano1969).

For grain size analysis, sediment samples were manually homogenized, dried at 60 °C until achieving a constant weight, and sieved to determine percent mass of grain size fractions (ASTM D6913-04). Percent OM was determined by loss on ignition after combustion in a muffle furnace at 500 °C for four hours (Heiri et al. 2001). C:N content was measured on acid-rinsed (10% HCl) subsamples of sediment from Whirl-Pak bags using a PDZ Europa ANCA-GSL elemental analyzer at the UC Davis Stable Isotope Facility.

Porewater for sulfide analysis was collected using Rhizon CSS samplers (Rhizosphere Research Products) in the field to extract porewater by capillary action. 60 mL syringe cores were used to collect intact sediment cores from each site, leaving a few centimeters of overlying water to minimize oxygen exposure to sediments. The Rhizon was inserted into the top of each 60 mL syringe core until about 8 mL of porewater was extracted into vacuum sealed test tubes. 10 µL of potassium hydroxide and 10 µL of zinc acetate were added immediately in the field to prevent sulfide oxidation. In the lab, sulfide samples were measured spectrophotometrically using the methylene blue method, with standards prepared by bubbling with Argon (Standard Methods 4500-S2-D).

Percent cover of macroalgae and seagrass was estimated at each of the sampling sites using a 0.25 m^2 quadrat subdivided into 10 cm by 10 cm squares. Visual estimates were made at three haphazardly determined locations within each sampling site. In addition, three cores (182.65 cm^2, PVC corer) were collected to measure biomass of drift macroalgae and seagrass. Samples were sorted into macroalgae, above and belowground biomass of seagrass, and detritus. Sorted samples were dried at 60 °C until achieving a constant weight to obtain dry biomass.

Subsamples of dried biomass were rinsed in 10% HCl to remove carbonates, and pulverized samples were shipped to the UC Davis Stable Isotope Facility. Samples were analyzed using a PDZ Europa ANCA-GSL elemental analyzer to determine natural abundance of ^{15}N and C and N content of the tissues.

Continuous Flow Incubation System

Intact sediment cores (7.6 cm diameter, ~15-20 cm height) were collected in seagrass beds with (+M) and without (-M) macroalgae cover (6 cores per site). Aboveground seagrass biomass was excluded from intact cores by gently parting the blades and manually inserting the core into the sediment. Cores with macroalgae were taken in areas of seagrass beds with 100% cover of macroalgae at least 10 cm thick. Seagrass and macroalgae were gently parted, and the core was inserted into the sediment. Immediately after extracting the core, macroalgae was placed on top of the sediment in the core (about 2-3 g wet mass). Cores were sealed and maintained in the dark at ambient temperatures during transport to the lab. 120 L of site water was collected and used to incubate the cores using a continuous-flow incubation system for three days (Lavrentyev et al. 2000;Gardner and McCarthy 2009).

Cores were wrapped in aluminum foil to prevent photosynthetic production of oxygen and fitted with a plunger containing inflow and outflow lines of gas impermeable PEEK tubing (0.040 IDx1/16OD, Western Analytical Products). The plunger was positioned with the inlet tubing approximately 1-2 cm above the sediment surface. Site water was held in aerated reservoirs and pumped over the sediment surface of intact cores at approximately 1.25 mL min^{-1} by peristaltic pumps (Fig. 5).

Two inflow reservoirs were enriched with $Na^{15}NO_3$ and two with $^{15}NH_4Cl$ to a final concentration of 50 µM and 10 µM, respectively. Each inflow reservoir flowed into two sediment cores; thus, two sediment cores from each site received unamended inflow water with no tracer additions, two cores received inflow water amended with 10 µM $^{15}NH_4^+$, and two cores received inflow water amended with 50 µM $^{15}NO_3^-$. Cores were allowed to equilibrate for 12-14 h before duplicate samples from inflow and outflow reservoirs were collected for nutrients (OP, NH_4^+, NO_2^-, NO_3^-, and urea), isotopically labeled $^{15}NH_4^+$, and dissolved gases ($^{28,29,30}N_2$, O_2, and Ar) once daily, for three days. Nutrient samples were filtered immediately to 0.2 µm into 15 mL plastic tubes and frozen. $^{15}NH_4^+$ samples were filtered using 0.2 µm syringe filters into 12 mL Exetainers (Labco Exetainers), leaving no head space. Dissolved gas samples were collected in

Exetainers, allowing the tubes to overflow for at least two volumes before collection, preserved with 200 µL of 50 % (w/w) zinc chloride, and stored at a temperature below ambient to prevent degassing prior to analysis. Nutrient samples were analyzed using the Lachat Quickchem 8500, while dissolved gases (Kana et al. 1994) and $^{15}NH_4^+$ (OXMIMS, Yin et al. 2014) were measured using membrane inlet mass spectrometry (MIMS). All nutrient and gas fluxes were calculated based on the flow rate, cross-sectional core area, and concentration differences between inflow and outflow (Lavrentyev et al. 2000).

$$\text{Flux} = \frac{(Co - Ci) \text{ x } f}{a}$$

Where *Co* is the outflow concentration (µM), *Ci* is the inflow/reservoir concentration, *f* is the flow rate (1.25mL min^{-1}), and *a* is the cross-sectional area of the core (0.0045 m^2). Flux calculations can be negative, indicating solute movement from the overlying water into the sediment core, or positive, indicating production and release from the sediments to overlying water (Lavrentyev et al. 2000; McCarthy et al. 2015).

$^{28}N_2$ was used to assess the relative balance between N fixation and denitrification/anammox occurring in unamended cores, while potential denitrification and calculated N fixation were determined from the $^{28,\ 29,\ \text{and}\ 30}N_2$ fluxes in $^{15}NO_3^-$ cores (An et al. 2001). Possible anammox was estimated from production of $^{29}N_2$ in $^{15}NH_4^+$ addition cores (Rysgaard et al. 2004). Nitrification was not prevented from occurring in these cores, so $^{29}N_2$ production cannot be excluded as an end-product of denitrification occurring with $^{14}NO_3^-$ already present within the incubation system combined with $^{15}NO_3^-$ produced via nitrification of added $^{15}NH_4^+$ (McCarthy et al. 2015). Potential DNRA was measured from $^{15}NH_4^+$ produced from added $^{15}NO_3^-$ (An and Gardner 2002). Since cation exchange mechanisms in sediments may interfere with $^{15}NH_4^+$ versus $^{14}NH_4^+$ measurements in $^{15}NO_3^-$ additions cores (Gardner et al. 1991), nitrate-induced ammonium flux (NIAF) was calculated as an additional proxy for DNRA. NIAF was calculated by subtracting total NH_4^+ flux in unamended cores from the total NH_4^+ flux in $^{15}NO_3^-$ cores (McCarthy et al. 2016).

Statistical Analysis

Statistical analysis was completed using SPSS (IBM) software. Data was tested for normality and was not normally distributed, so all correlations were conducted using Spearman's

Rho correlation coefficients (r^2). Biomass and sediment chemistry data was analyzed using the Kruskal-Wallis test to determine if data from sites +M and -M were significantly different from each other. For analysis all nutrient and dissolved gas fluxes, a Kruskal-Wallis univariate analysis of variance on ranked data was used to determine the main and interactive effects of macroalgae, treatment, and incubation. For all statistically significant main effects, a Post Hoc Test, Tukey HSD, was used to determine significance. Main effects indicate whether there was a significant effect of treatment, incubation date, or presence of algae independent of other factors. For interactive effects, where the effect of one variable depends on one or more other variables, 95% confidence intervals around estimated marginal means were used to determine significant differences among combinations of factors. It is important to note that if there were interactive effects, main effects of the individual variables in the interaction were not reported, because the effect was not consistent across levels of the other factors (incubation date, treatment, or presence of macroalgae).

Results

Water Column and Site Characteristics

Salinity varied across all sites and dates, and no clear seasonal trends were found for ambient nutrient concentrations across St. Joseph Bay (Table 1). Ambient NO_3^- concentrations were below detection limit on all dates and sites except on June 4 at +M and -M. Ambient NH_4^+ concentrations ranged from 0.93 ± 0.04 to 4.16 ± 0.02 µM, while OP and NO_2^- concentrations all remained under 1 µM. Urea concentrations were also all under 1 µM, except on June 18 at site NM1.

Biomass data (Table 2) and sediment chemistry (Table 3) varied across sites and dates. Notable correlations for macroalgae sites were that sulfide concentrations were positively correlated to seagrass shoot density (r^2= 0.639, p = 0.01). For no macroalgae sites, sulfide concentrations were also correlated to shoot density (r^2=0.825, p =0.01), as well as porewater NH_4^+ (r^2=-0.586, p =0.01). Also, % OM was correlated to seagrass aboveground biomass (r^2=0.741, p =0.01) and shoot density (r^2=0.530, p =0.05) in no macroalgae areas.

Site characteristics were compared between the three sites with macroalgae blooms (+M, M1, M2) and three sites with no macroalgae blooms (-M, NM1, NM2) to establish possible chemical and physical differences. On June 4, the only differences detected between macroalgae

and no macroalgae sites were higher porewater sulfide concentrations (p =0.011) and % cover of macroalgae (p =0.002) at macroalgae sites. On June 18, aboveground seagrass biomass (p =0.019), belowground seagrass biomass (p =0.007), and % cover of seagrass (p =0.035) was significantly greater in areas with no macroalgae. On June 18 areas with macroalgae had significantly greater macroalgae biomass (p <0.001), and % cover of macroalgae (p <0.01) than no macroalgae areas. On June 26, aboveground seagrass biomass (p =0.038) and belowground seagrass biomass (p =0.015) were greater in areas with no macroalgae, while areas with macroalgae had higher macroalgae biomass (p <0.001), sulfide concentrations (p =0.004) and % cover of macroalgae (p =0.008).

Sediment oxygen and nutrient fluxes

Sediment Oxygen Demand (SOD)

Cores with drift macroalgae had significantly greater SOD than no macroalgae cores (p <0.001), with no effect of treatment and no interactive effects. Across all incubations and treatments (unamended, $^{15}NH_4^+$, and $^{15}NO_3^-$ additions), average SOD in macroalgae cores was 2587.87 ± 96.33 µmol O_2 m^{-2} hr^{-1} compared to 1566.06 ± 80.18 µmol O_2 m^{-2} hr^{-1} in no macroalgae cores (Table 4, Fig. 6). SOD was also significantly greater on June 18 than June 26 (p =0.001); however, other comparisons of SOD across incubations and treatments were not significant. In $^{15}NH_4^+$ addition cores with no macroalgae, SOD was positively correlated to possible anammox and $^{29}N_2$ flux (r^2=0.571, p =0.05), and in $^{15}NO_3^-$ addition cores with no macroalgae, SOD was positively correlated to potential DNRA (r^2=0.727, p =0.01).

Nutrient Fluxes

Mean NH_4^+ flux in all macroalgae cores (24.76 ± 12.29; all nutrient fluxes measured in µmol N m^{-2} hr^{-1} or µmol P m^{-2} hr^{-1} for OP ± standard error) was significantly lower than the mean for all no macroalgae cores (77.41 ± 11.13) (p <0.001) (Fig. 7). Sampling date influenced NH_4^+ flux with June 4 being significantly higher than June 18 (p <0.001) and June 26 (p =0.019). For treatment, average NH_4^+ flux for $^{15}NO_3^-$ enriched cores was 109.30 ± 15.98 compared to 31.34 ± 9.91 in unamended cores (p <0.001) and 12.62 ± 13.43 in $^{15}NH_4^+$ enriched cores (p <0.001). For the effects of the $^{15}NO_3^-$ addition in unamended cores with macroalgae, there was a positive correlation between NH_4^+ and NO_3^- fluxes (r^2=0.571, p =0.05).

NO_2^- fluxes were only significantly affected by treatment (p <0.001), but not incubation or presence of macroalgae. Average NO_2^- fluxes for +M and -M in $^{15}NO_3^-$ enriched cores across the three incubations were 47.62 ± 6.40 compared to -1.60 ± 0.97 in unamended cores (p <0.001) and 0.02 ± 0.36 in $^{15}NH_4^+$ enriched cores (p <0.001). (Table 4; Fig. 8).

Treatment and incubation significantly influenced NO_3^- fluxes (both p <0.001; Fig. 9). Including all treatments, June 26 had lower NO_3^- fluxes than June 4 (p <0.001) and June 18 (p =0.001). $^{15}NO_3^-$ addition cores stimulated NO_3^- uptake by sediments with an average NO_3^- flux of -245.49 ± 18.88, which was significantly different from 0.86 ± 0.89 in $^{15}NH_4^+$ enriched cores (p <0.001) and 0.52 ± 0.78 in unamended cores (Table 4; Fig. 9).

There were significant interactive effects between macroalgae and incubation (p =0.014) for OP fluxes. All average OP fluxes were negative, but no other significant differences or trends occurred over the three incubations, or between treatments for +M and -M cores (Table 4; Fig. 10).

Urea fluxes were influenced by interactive effects between macroalgae and incubation (p =0.011), with no effect of treatment. On June 4, urea flux was significantly greater in -M cores than +M cores (3.62 ± 1.84, -3.90 ± 2.27, respectively) but this difference was not observed in the other incubations (Table 4; Fig. 11).

N transformations

Net $^{28}N_2$ Flux

There were significant interactive effects between incubation and treatment (p <0.001) as well as macroalgae and incubation (p =0.026) on net $^{28}N_2$ fluxes. The effect of macroalgae changed over different incubations. In all +M cores, June 26 (-10.27 ± 7.43) was significantly different than June 4 (-82.95 ± 17.14) and June 18 (-51.432 ± 12.91) (Table 4).The effect of treatment changed over the course of three incubations. For unamended +M and -M cores, June 26 and June 18 were significantly different from each other (p =0.007). In $^{15}NH_4^+$ addition +M and -M cores, June 26 had lower $^{28}N_2$ fluxes than both June 4th and June 18th. In $^{15}NO_3^-$ cores, there were no significant differences between incubations.

Averages for $^{28}N_2$ flux were predominantly negative across all incubations (Fig. 12). The changing effect of macroalgae, depending on incubation shows that there was a change from

being a net $^{28}N_2$ sink on June 4 and June 18 to being neither a sink nor source of $^{28}N_2$ during the last incubation on June 26.

Other N pathways

Potential denitrification rates, measured by total $^{28+29+30}N_2$ production in $^{15}NO_3^-$ cores, averaged 12.02 ± 4.52 in +M cores and 17.19 ± 4.22 in -M cores across all three incubations (Fig. 14, A). Potential DNRA rates, measured as $^{15}NH_4^+$ production from $^{15}NO_3^-$, averaged 12.36 ± 5.21 in +M cores and 19.55 ± 3.90 in -M cores across all three incubations (Fig. 14, B). In $^{15}NO_3^-$ addition, +M cores, NO_2^- flux was correlated to potential DNRA (r^2=0.595, p =0.01) and calculated N fixation (r^2=0.558, p =0.05). Potential DNRA and potential denitrification were also negatively correlated (r^2=-0.666, p =0.01). NIAF, calculated as the difference between NH_4^+ flux in $^{15}NO_3^-$ and unamended cores, averaged 63.45 ± 16.59 in +M cores and 97.44 ± 13.98 in -M cores (Fig. 14, D). In $^{15}NO_3^-$ addition, -M cores, potential DNRA was correlated positively to NO_2^- flux (r^2=0.527, p =0.05) and potential DNF (r^2=0.477, p =0.05). Calculated N fixation, based on production of heavy isotope and balance with oxygen ratio (An et al. 2001), averaged 21.78 ± 10.46 in macroalgae cores and 5.12 ± 7.66 in no macroalgae cores (Fig. 14, C). There were no statistically significant trends found between +M and -M cores, or across sampling dates for potential DNF, potential DNRA, N fixation, and NIAF.

Discussion

St. Joseph Bay is a relatively unimpacted coastal system with continuous *T. testudinum* beds along the margin of the bay and seasonal drift macroalgae blooms, providing a study site to determine how drift macroalgae may affect the fate of N in seagrass ecosystems. Previous research led to the hypothesis that seagrass beds with or without drift macroalgae cover would have greater rates of denitrification than DNRA because denitrification is more energetically favorable than DNRA. Previous research also led to the hypothesis that areas with drift macroalgae cover would have greater DNRA rates than seagrass beds with no drift macroalgae, likely due to higher % OM and sulfide concentrations associated with macroalgae cover and lastly, literature also supported the idea that N cycling rates would change over the duration of the drift macroalgae bloom due to chemical differences imposed by newly established macroalgae blooms versus decomposing macroalgae on sediments. The results show that drift macroalgae blooms within St. Joseph Bay did not significantly affect the majority of N

transformation pathways, but the rates measured in this study may be important in the context of larger seasonal trends, as compared to N rates measured within St Joseph Bay and other seagrass beds.

DNRA represents recycling of bioavailable NH_4^+ within sediments (Burgin and Hamilton 2007). DNRA was stimulated in $^{15}NO_3^-$ addition cores, but there were no significant differences in potential DNRA between +M and -M cores. N removal pathways from sediments include anammox (Mulder et al. 1995) and denitrification (Seitzinger 1988). Average potential denitrification rates in -M cores was not significantly different than +M cores. But, potential denitrification rates were an order of magnitude greater than possible anammox in +M and -M cores (Fig. 14, A; Fig. 13). Possible anammox, $^{29}N_2$ production in $^{15}NH_4^+$ addition cores, was significantly higher in +M than -M cores, but anammox rates represented less than 2% of total N removal. The primary N removal pathway was through denitrification, rather than anammox, in seagrass sediments of St. Joseph Bay during June 2017, regardless of the presence of drift macroalgae. Low NO_3^- ambient concentrations at all sites (most below detection limit) suggests at first that denitrifying bacteria were possibly NO_3^- limited at all sites, however, there was a lack of $^{29}N_2$ and $^{30}N_2$ production in $^{15}NO_3^-$ addition cores, supporting that coupled nitrification-denitrification was occurring more than direct denitrification.

Sulfide levels are thought to inhibit denitrification and promote DNRA (Burgin and Hamilton 2007). Even though sulfide levels at macroalgae sites were significantly higher than no macroalgae sites during June 4 and June 26, there were no significant differences in potential denitrification or potential DNRA between macroalgae and no macroalgae cores. Also, % OM was not different between areas with and without drift macroalgae across the bay, though +M sites did have significantly greater % OM than -M sites across all incubations (p <0.001). Previous research has shown that there may not be a significant amount of OM from degrading macroalgae blooms that gets incorporated into sediments (Sundbäck et al. 1990), though other studies have shown that OM from macroalgae may contribute up to half of the annual OM deposited in coastal sediments (Kautsky 1995). This altogether suggests that instead of just % OM or sulfide levels, possibly the lability of OM, has more control on the preference of denitrification versus DNRA rates (Burgin and Hamilton 2007). SOD was also greater in +M than -M, supporting indirectly that sediment metabolism was increased in areas with macroalgae, and may be why denitrification was favored (Cornwell et al.1999). Other research has shown

that macroalgae mats can shift the microbenthic community from diatom dominated to cyanobacterial dominated, shifting sediments to net heterotrophy and increasing SOD (Garcia-Robledo and Crozo 2011).

Denitrification rates in this study were lower than previously measured rates using the continuous-flow incubation method in St. Joseph bay by Hoffman et al. (unpublished) during August 2012 and July 2014, which ranged from 89–221 μmol N m^{-2} h^{-1} and 127–284 μmol N m^{-2} h^{-1}, respectively. However, data showing that anammox was not a significant source of NO_2^- removal in St. Joseph seagrass beds was similar to Hoffman et al. (unpublished) findings. Denitrification rates from this study were higher than seagrass sediments in Australia measured using sediment slurries by Salk et al. 2017 (0.16 μmol N m^{-2} h^{-1}), while anammox rates from this study were similar to their bare sediments (0.18 μmol N m^{-2} h^{-1}) but not seagrass sediments (0.60 μmol N m^{-2} h^{-1}). Denitrification rates in this study were also lower than rates measured in other seagrass beds in Australia (29.2–445.2 μmol N m^{-2} hr^{-1}; Eyre et al. 2013) and *T. testudinum* beds in Texas (16 μmol N m^{-2} h^{-1}; An and Gardner 2002), but, were similar to average denitrification rates in *Zostera marina* beds (17.5 μmol N m^{-2} h^{-1}; Aoki and McGlathery 2017).

Potential DNRA rates were greater than Australian seagrass beds from Salk et al. 2017 (<1 μmol N m^{-2} hr^{-1}) but less than rates measured in *T. testudinum* beds in Laguna Madre, Texas (69 μmol N m^{-2} hr^{-1}; An and Gardner 2002), and in previous incubations in St. Joseph Bay (average ~30-40 μmol N m^{-2} hr^{-1}; Hoffman et al. unpublished). If potential DNRA rates are an underestimate due to cation exchange mechanisms in sediments (e.g., Gardner and Seitzinger 1991), NIAF averages in +M and -M cores (Fig. 14, D) would need to be used in place of DNRA rates. The concept of NIAF has been applied in other seagrass sediments within St. Joseph Bay (~300 μmol N m^{2-1} hr-1; Hoffman et al. unpublished) as well as in Texas (262 μmol N m^{2-1} hr^{-1}; Gardner et al. 2006). NIAF rates were not significantly different between +M and -M and rates of DNRA were still lower than previously measured rates, but, the overall magnitude of recycled N would then be greater than removed N (via denitrification and anammox) in sediments. There are no known studies measuring N transformation pathways under drift macroalgae blooms in seagrass beds, making it unclear whether the lack of difference between macroalgae and no macroalgae areas is consistent with other studies.

Besides the importance of removal and recycling of N in sediments, the transformation of N_2 into NH_4^+ via N fixation, is an important source of N for many bacteria and phytoplankton

(Knapp 2012). Seagrass bed sediments contribute about 10% of total sediment marine N fixation, even though they comprise about 0.1% of total marine area (Capone 1983). Average N fixation calculations from macroalgae and no macroalgae cores were not significantly different but suggest that N fixation is occurring simultaneously with denitrification in these sediments. $^{28}N_2$ fluxes were negative in our unamended cores (Figure 12), showing that N fixation was occurring at higher rates than denitrification. There were mixed effects of macroalgae on $^{28}N_2$ fluxes, but overall, from June 4 to June 26, N fixation rates and $^{28}N_2$ fluxes decreased, showing a switch from sediments being a net N sink to neutral. This decrease in N fixation, and previous research showing no heterotrophic N fixation in St. Joseph Bay during July and August (Hoffman et al. unpublished), possibly showing that higher N fixation rates from this study may be a part of larger seasonal trends. Research in sediments of Narragansett Bay, RI showed that when there is less organic matter reaching sediments, there is a switch from net denitrification to N fixation, typical of seasonal trends from increased nutrients after remineralization of algae blooms during the winter-spring (Fulweiler et al. 2007). In St. Joseph Bay, there is potentially less OM during spring when drift macroalgae blooms have not degraded and seagrasses are not as productive, leading to higher N fixation rates than in the summer when OM to sediments is greater, leading to greater denitrification rates.

N fixation in marine and other ecosystems is often inhibited by inorganic N, though many coastal sediments often have high concentrations (100-200 µM) of NH_4^+ present with high rates of N fixation (Welsh et al. 2000). N fixation may be able to proceed in NH_4^+ rich sediments because there are other controlling environmental factors, such as organic carbon source and oxygen concentrations (McGlathery et al. 1998), or that N fixation can help bacteria balance their redox potential with excess electrons provided from N fixation (Tichi and Tabita, 2000). There are few studies examining N fixation rates in seagrass sediments, and further interpretation of how NH_4^+ concentrations, or other environmental factors, could affect N fixation rates in these sediments are even fewer (Knapp 2012, Welsh et al. 2000). Porewater NH_4^+ in seagrass beds in St. Joseph Bay ranged from 312.90 ± 57.16 to over 716.01 ± 81.13 µM, and sediment % OM ranged from 0.49% to 6.08%. It is also important to note that sediment heterogeneity can occur at small scales, and measurements for *in situ* porewater NH_4^+ are often influenced by sampling procedures, e.g. leakage of NH_4^+ from damage to the rhizosphere (Hansen and Lomstein 1999).

Rates of N fixation have ranged from 0.09 to 416.67 μmol N m^{-2} hr^{-1} in seagrass beds (Welsh et al. 2000) and are seasonally dependent for temperate seagrass beds (e.g., McGlathery et al. 1998), showing that N fixation rates from this study fall within the ranges reported by others, even in the presence of high porewater NH_4^+ concentrations in St. Joseph Bay.

It is also important to consider methodologies when comparing N transformation rates. Sediment slurry techniques disrupt natural redox gradients in sediments and may overestimate N rates in vegetated sediments due to disturbing *in situ* plant tissues, which may release DIN and organic carbon that would usually not be as readily available to microbes (e.g., Hansen and Lomstein 1999). The acetylene block technique for denitrification measurements specifically inhibits N fixation, has been shown to inhibit denitrifiers, nitrifiers, and other reducing bacteria (Taylor 1983), while producing ethylene, a compound that can affect a variety of microorganisms (Capone 1988).

The main weakness of this study is the lack of temporal resolution, with only three incubations (June 4, 18, and 26, 2017) and that our sediment chemistry samples are not paired directly with our incubation cores. In this study, sampling and porewater measurements were from bulk sediment samples, so direct interpretation and connection of our sediment chemistry to N transformation rates, or extrapolation of N rates across the bay, is inherently complicated. This study represents the first time that living macroalgae was added to intact sediment cores for the continuous-flow incubation method. Though the cores were wrapped in foil to prevent photosynthetic activity, and no oxygen bubbles were detected to influence N transformation rates, there are possible methodological issues that may have been undetected due to dark respiration of drift macroalgae.

Based on our data from the continuous-flow incubation method, the magnitude of N recycling (DNRA) and formation of bioavailable N (N fixation) was equal or greater than our N removal pathways (anammox and denitrification) in June 2017 in seagrass beds with and without drift macroalgae blooms. The rates presented in this study differ from N transformation rates measured by Hoffman et al. (unpublished) in St. Joseph Bay during August 2012 and July 2014. Though the original hypotheses in this study were not consistently supported, baseline data for N cycling in seagrass beds, as well as understanding chemically what happens under drift macroalgae blooms, remains important. With the increasing amount of anthropogenic N reaching coastal ecosystems, understanding how N loading may affect seagrasses and other coastal

habitats, which are ecologically important for many fish and invertebrates, is imperative. Drift macroalgae blooms negatively affect seagrasses, and macroalgae blooms are increasing world-wide as a result of nutrient loading, but no known studies have evaluated how drift macroalgae may alter N cycling in these systems. To mitigate the possible effects of these increasing loads, providing baseline data on sediment N transformations is an important first step in understanding these effects.

Integration of the Thesis Research

Nutrient loading often has cascading affects in ecosystems, altering biological and chemical interactions of microbes to macro-flora and -fauna, often having negative ecological implications such as increasing drift macroalgae blooms. Though N cycling is microbial mediated, many temporal and environmental factors can influence N transformation rates and pathways. The project described is integrative in nature and broadly determined how macroalgae can affect not only N cycling rates and pathways, but also general sediment chemistry, water column nutrients, microbial community activity, and effects on seagrass community in the context of N cycling in St. Joseph Bay, FL.

References

An S, Joye SB. 2001. Enhancement of coupled nitrification-denitrification by benthic photosynthesis in shallow estuarine sediments. Limnol Oceanogr. 46(1): 62-74.

An S, Gardner WS. 2002. Dissimilatory nitrate reduction to ammonium (DNRA) as a nitrogen link, versus denitrification as a sink in a shallow estuary (Laguna Madre/Baffin Bay, Texas). Marine Ecology Progress Series 237:41-50.

Aoki LR, McGlathery KJ. 2017. Push-pull incubation method reveals the importance of denitrification and dissimilatory nitrate reduction to ammonium in seagrass root zone. Limnol Oceanogr Methods. 15:766-781.

Arroyo NL, Bonsdorff E. 2016. The role of drifting algae for marine biodiversity. -in E. Olafsson (ed.): Marine macrophytes as foundations species. CRC Press, Taylor and Francis Group pp. 285.

Asmus RM, Sprung M, Asmus H. 2000. Nutrient fluxes in intertidal communities of a South European lagoon (Ria Formosa) – similarities and differences with a northern Wadden Sea bay (Sylt-Rømø Bay). Hydrobiologia. 2000. 436: 217.

ASTM D6913 - 04e1.2009. Standard Test Methods for Particle-Size Distribution (Gradation) of Soils Using Sieve Analysis.

Beck MW, Heck Jr. KL, Able KW, Childers DL, Eggleston DB, Gillanders BM, Halpern B, Hays CG, Hoshino K, Minello TJ, Orth RJ, Sheridan PF, Weinstein MP. 2001. The identification, conservation, and management of estuarine and marine nurseries for fish and invertebrates. BioScience. 51(8): 633-641.

Bell SS, Hall MO. 1997. Drift macroalgal abundance in seagrass beds: investigating large-scale associations with physical and biotic attributes. Marine Ecology Progress Series 147: 277-283.

Beman M, Arrigo R, Kevin A, Matson P.2005. Agricultural runoff fuels large phytoplankton blooms in vulnerable areas of the ocean. Nature. 434: 211-214.

Boesch DF, Boynton WR, Crowder LB, Diaz RJ, Howarth RW, Mee LD, Nixon SW, Rabalais NN, Rosenberg R, Sanders JG, Scavia D, Turner RE. 2009. Nutrient enrichment drives Gulf of Mexico hypoxia. EOS 90: 117–119.

Burgin AJ, Hamilton SK. 2007. Have we overemphasized the role of denitrification in aquatic ecosystems? A review of nitrate removal pathways. Frontiers in Ecology and the

Environment 5:89-96.

Capone DG, Carpenter EJ.1982. Nitrogen fixation in the marine environment. Science. 217 (4565):1140-2.

Cebrian J, Corcoran D, Lartigue J. 2014. Eutrophication-Driven Shifts in Primary Producers in Shallow Coastal Systems: Implications for System Functional Change. Estuaries and Coasts. 37: S180-S187.

Coastal and Estuarine Studies Interactions between Macro-and Microorganisms in Marine Sediments. Ed. Erik Kristensen, Ralf R. Haese, and Joel E. Kostka. New York: American Geophysical Union, 2005. 7-30.

Cornwell JC, Kemp WM, Kana TM. 1999.Denitrification in Coastal Ecosystems: Methods, Environmental Controls, and Ecosystem Level Controls, a Review, Aquatic Ecology. 33: 41-54.

Corzo A, Van Bergeijk SA, García-Robledo E. 2009. Effects of green macroalgal blooms on intertidal sediments: net metabolism and carbon and nitrogen contents. Marine Ecology Progress Series. 380: 81–93.

Duarte CM, Middleburg JJ, Caraco N. 2005. Major role of marine vegetation on the oceanic carbon cycle. Biogeosciences. 2:1-8.

Eyre BD, Maher D, Oakes JM, Erler DV, Glasby TM. 2011. Differences in benthic metabolism, nutrient fluxes, and denitrification in Caulerpa taxifolia communities compared to uninvaded bare sediment and seagrass (*Zostera capricorni*) habitats. Limnology and Oceanography. 56(5):1737-1750.

Eyre BD, Maher DT, Squire P. 2013. Quantity and quality of organic matter (detritus) drives N2effluxes (net denitrification) across seasons, benthic habitats, and estuaries. Global Biogeochemical Cycles. 27(4):1083-1095.

Florida Department of Environmental Protection. 2001a. Seagrass and the economy. Retrieved February 13, 2006, from Office of Coastal and Aquatic Managed Areas Website: http://www.dep.state.fl.us/coastal/habitats/seagrass/awareness/economy.htm.

Fonseca MS, Fisher JS. 1986. A comparison of canopy friction and sediment movement between four species of seagrass with reference to their ecology and restoration. Marine Ecology Progress Series. 29:15-22.

Fourqurean JW, Zieman JC. 2002. Nutrient content of the seagrass *Thalassia testudinum*

reveals regional patterns of relative availability of nitrogen and phosphorus in the Florida Keys USA. Biogeochemistry. 61:229-245.

Francis CA, Beman JM, Kuypers MM. 2007. New processes and players in the nitrogen cycle: the microbial ecology of anaerobic and archaeal ammonia oxidation. ISME J. 1(1):19-27.

Frederiksen MS, Glud RN. 2006. Oxygen dynamics in the rhizosphere of *Zostera marina*: a two-dimensional planar optode study. Limnology and Oceanography. 51(2):1072-1083.

Fulweiler RW, Nixon SW, Buckley BA, Granger SL. 2007. Reversal of the net dinitrogen gas flux in coastal marine sediments. *Nature.* 448: 180–182.

Fulweiler RW, Brown SM, Nixon SW, Jenkins BD. 2013. Evidence and a conceptual model for the co-occurrence of nitrogen fixation and denitrification in heterotrophic marine sediments. Marine Ecology Progress Series. 482: 57–68.

Galloway J, Aber J, Erisman J, Seitzinger S, Howarth R, Cowling E, Cosby B. 2003. The nitrogen cascade. BioScience 53: 341–356.

García-Robledo E, Corzo A, de Lomas JG, Van Bergeijk SA. 2008. Biogeochemical effects of macroalgal decomposition on intertidal microbenthos: a microcosm experiment. Marine Ecology Progress Series. 356: 139-151.

García-Robledo E, Corzo A. 2011. Effects of macroalgal blooms on carbon and nitrogen biogeochemical cycling in photoautotrophic sediments: an experimental mesocosm. Marine Pollution Bulletin. 62: 1550–1556.

Gardner WS, McCarthy MJ, S. An, D. Sobolev, K.S. Sell, and D.Brock. 2006. Nitrogen fixation and dissimilatory nitrate reduction to ammonium (DNRA) support nitrogen dynamics in Texas estuaries. Limnology and Oceanography. 51: 558–568.

Gardner WS, McCarthy MJ. 2009. Nitrogen dynamics at the sediment-water interface in shallow, subtropical Florida Bay: Why denitrification efficiency may decrease with increased eutrophication. Biogeochemistry. 95: 185–198.

Gardner WS, Seitzinger S, Malczyk JM. 1991. The effects of sea salts on the forms of nitrogen released from estuarine and freshwater sediments: Does ion pairing affect ammonium flux? Estuaries. 14(2):157-166.

Giblin AE, Tobias CR, Song B, Weston N, Banta GT, Rivera-Monroy VH. 2013. The importance of dissimilatory nitrate reduction to ammonium (DNRA) in the nitrogen cycle

of coastal ecosystems. Oceanography. 26(3):124–131.

Hansen JW, Lomstein BA. 1999. Leakage of ammonium, urea, and dissolved organic nitrogen and carbon from eelgrass Zostera marina roots and rhizomes during sediment handling. Aquat Microb Ecol. 16:303-307.

Hatton D, Pickering WF. 1990. Modified procedure for the determination of exchangeable ammonium ions in lake sediments. Chemical Speciation and Bioavailability. 2(4):139-147.

Hauxwell J, Cebrian J, Valiela I. 2003. Eelgrass *Zostera marina* loss in temperate estuaries: Relationship to land-derived nitrogen loads and effect of light limitation imposed by algae. Marine Ecology Progress Series. 247: 59–73.

Heck Jr. KL, Pennock JR, Valentine JF, Coen LD, Sklenar SA. 2000. Effects of nutrient enrichment and small predator density on seagrass ecosystems: An experimental assessment. Limnology and Oceanography. 5.

Heisler J, Glibert PM, Burkholder JM, Anderson DM, Cochlan W, Dennison WC, Dortch Q, Gobler CJ, Heil CA, Humphries E, Lewitus A, Magnien R, Marshall HG, Sellner K, Stockwell DA, Stoecker DK, Suddleson M. 2008. Eutrophication and harmful algal blooms: a scientific consensus. Harmful Algae. 8: 3–13.

Heiri, O, Lotter, A, Lemcke, G. 2001. Loss on Ignition as a Method for Estimating Organic and Carbonate Content in Sediments: Reproducibility and Comparability of Results. Journal of Paleolimnology. 25.

Hemminga MA, Duarte CM. 2000. Seagrass Ecology Cambridge University Press.

Hoffman D, Mutchler T, McCarthy MJ, Newell SE, Gardner WS. 2015. Comparing nitrogen transformation rates in vegetated and unvegetated marine sediments of St. Joseph Bay, FL. Assoc for the Sci of Limnol and Oceanogr. Aquatic Sciences Meeting, Granada, Spain. 22-27 February 2015.

Holmquist JG. 1997. Disturbance and gap formation in a marine benthic mosaic; influence of shifting macroalgal patches on seagrass structure and mobile invertebrates. Mar. Ecol. Prog. Ser. 158: 121–130.

Holmer M, Hasler-Sheetal H. 2014. Sulfide intrusion in seagrasses assessed by stable sulfur isotopes—a synthesis of current results. Front. In Mar. Sci. 1:64.

Joye SB, Anderson IC. 2008. Nitrogen cycling in coastal sediments. Nitrogen in the

marine environment, 2nd edn. Academic Press, Amsterdam, pp.868-915.

Kana TM, Darkangelo C, Hunt MD, Oldham JB, Bennett GE, Cornwell JC. 1994. Membrane inlet mass spectrometer for rapid high-precision determination of N2, O2, and Ar in environmental water samples. Analytical Chemistry. 66:4166-4170.

Kautsky U. 1995. Ecosystem processes in coastal areas of the Baltic Sea. PhD Thesis, Stockholm University.

Koch MS, Erskine JM. 2001. Sulfide as a phytotoxin to the tropical seagrass *Thalassia testudinum*: interactions with light, salinity, and temperature. J. Exp. Mar. Biol. Ecol. 266: 81—95.

Knapp A. 2012. The sensitivity of marine N2 fixation to dissolved inorganic nitrogen. Front. Microbiol. 3.

Koch EW. 1999. Sediment resuspension in a shallow *Thalassia testudinum* bed. Aquat. Bot. 65: 269–280.

Lapointe EB. 1997. Nutrient thresholds for bottom-up control of macroalgal blooms on coral reefs in Jamaica and southeast Florida. Limnol Oceanogr. 45 (5, part 2): 1119-1131.

Lavrentyev P, Gardner WS, Yang L. 2000. Effects of the Zebra mussel on microbial composition and nitrogen dynamics at the sediment-water interface in Saginaw Bay, Lake Huron. Aquat. Microb. Ecol. 21:187-194.

McCarthy MJ, Newell SE, Carini SA, Gardner WS. 2015. Denitrification dominates sediment nitrogen removal and is enhanced by bottom-water hypoxia in the northern Gulf of Mexico. Estuaries & Coasts. 38: 2279–2294.

McCarthy MJ, Gardner WS, Lehmann MF, Guindon A, Bird DF. 2016. Benthic nitrogen regeneration, fixation, and denitrification in a temperate, eutrophic lake: Effects on the nitrogen budget and cyanobacteria blooms. Limnol. Oceanogr. 61:1406-1423.

McGlalathery KJ, Risgaard-Petersen N, Christensen PB. 1998. Temporal and spatial variation in nitrogen fixation activity in the eelgrass *Zostera marina* rhizosphere. Mar. Ecol. Prog Ser. 168:245-258.

McGlathery KJ, Anderson IC, Tyler AC. 2001. Magnitude and variability of benthic and pelagic metabolism in temperate coastal lagoon. Marine Ecology Progress Series. 216:1–15.

McGlathery KJ, Sundback K, Anderson IC. 2007. Eutrophication, patterns in shallow coastal

bays and lagoons. Mar Ecol Prog Ser. 348:1–18.

McCarthy MJ, Gardner WS, Lehmann MF, Bird DF. 2013. Implications of water column ammonium uptake and regeneration for the nitrogen budget in temperate, eutrophic Missisquoi Bay, Lake Champlain (Canada/USA). Hydrobiologia. 718: 173–188.

Mulder A, van de Graaf AA, Robertson LA, Kuenen JG. 1995. Anaerobic ammonium oxidation discovered in a denitrifying fluidized bed reactor. FEMS Microbiol. Ecol.16: 177–184.

Littler, M.M, Littler, D.S., and Lapointe, B.E. 1986. Baseline studies of herbivory and eutrophication on dominant reef communities of Looe Key National Marine Sanctuary. NOAA Technical Memorandum. U.S. Government Printing Office. NOS MEMD 1.

National Ocean Service. 1988. Tidal benchmark sheets (ASC II format). Retrieved from National Oceanic Atmospheric Administration Website: http: www.nmfs.noaa.gov/fishwatch.

Orth RJ, Carruthers TJB, Dennison WC, Duarte CM, Fourqurean JW, Heck KL, Hughes AR, Kendrick GA, Kenworthy WJ, Olyarnik S, Short FT, Waycott M, Williams SL. 2006. A Global Crisis for Seagrass Ecosystems. BioScience. 56 (12):987–996.

Osterling, M. Pihl, L. 2001. Effects of filamentous green algal mats on benthic macrofaunal functional feeding groups. Journal of Experimental Marine Biology and Ecology 263: 159-183.

Payne WJ. 1973. Reduction of nitrogenous oxides by microorganisms. Bacteriol. Rev. 17: 409-452.

Pedersen MF, Borum J, Fotel FL. 2010. Phosphorus dynamics and limitation of fast- and slow-growing temperate seaweeds in Oslofjord, Norway. Marine Ecology Progress Series. 399: 103–115.

Pihl L, Svenson A, Moksnes PO, Wennhage H. 1999. Distribution of green algal mats throughout shallow soft bottoms of the Swedish Skagerrak archipelago in relation to nutrient sources and wave exposure. Journal Sea Res. 41: 281–294.

Robledo G, Corzo A. 2011. Effects of macroalgal blooms on carbon and nitrogen biogeochemical cycling in photoautotrophic sediments: an experimental mesocosm. Mar. Pollut. Bull. July:62-7.

Rysgaard S, Glud RN, Risgaard-Petersen N, Dalsgaard T. 2004. Denitrification and

anammox activity in Arctic marine sediments. Limnol. Oceanogr. 49: 1493–1502.

Salk KR, Erler DV, Eyre BD, Carlson-Perrett N, Ostrom NE. 2017. Unexpectedly high degree of anammox and DNRA in seagrass sediments: Description and application of a revised isotope pairing technique. Geochimica et Cosmochimica. 211:64-78.

Santschi P, Hohener P, Benoit G, Buchholtzten BM.1990. Chemical processes at the sediment-water interface. Mar. Chem. 30(269):3--5.

Seitzinger SP.1988. Denitrification in fresh-water and coastal marine ecosystems– Ecological and geo- chemical significance. *Limnol. Oceanogr.* 33: 702–724.

Smyth AR, Thomspon SP, Siporin KN, Gardner WS, McCarthy MJ, Piehler MF. 2013. Assessing nitrogen dynamics throughout the estuarine landscape. Estuaries and Coasts. 36:44-55.

Solórzano L. 1969. Determination of ammonia in natural waters by the phenol hypochlorite method. Limnology and Oceanography. 14(5):798-801.

Standard Methods Online -- Standard Methods for the Examination of Water and Wastewater. http://standardmethods.org/

Stewart RA, Gorsline DS. 1962. Recent sedimentary history of St. Joseph Bay, Florida. Sedimentology. 1:256-286.

Sundbäck K, Jönsson B, Nilsson P, Lindström I. 1990. Impact of accumulating drifting macroalgae on a shallow-water sediment system: an experimental study. Mar. Ecol. Prog. Ser. 58: 261–274.

Taylor BF. 1983. Assays of microbial nitrogen transformation. In *Nitrogen in the Marine Environment*. Ed. E.J. Carpenter and D.G. Capone. Academic Press, New York, pp. 809—837.

Tichi MA, Tabita FR. 2000. Maintenance and control of redox poise in *Rhodobacter capsulatus* strains deficient in the Calvin- Benson-Bassham pathway. *Arch. Microbiol.* 174: 322–333.

Tiedje JM, Sexstone AJ, Myrold DD, Robinson JA. 1982. Denitrification: ecological niches, competition and survival. Antonie Van Leeuwenhoek 48: 569–583.

Vitousek PM, Aber JD, Howarth RW, Likens GE, Matson PA, Schindler DW, Schlesinger WH, Tilman DG. 1997. Human alteration of the global nitrogen cycle: sources and consequences. Ecological Applications. 7: 737–750.

Wang Y, Wang Y, Zhu L, Zhou B, Tang X. 2012. Comparative studies on the ecophysiological differences of two green tide macroalgae under controlled laboratory conditions. Plos One. 7(8): 1–16.

Ward BB. 2008**.** Nitrification. In: Encyclopedia of Ecology. Eds. S. E. Jorgensen and B. D. Faith, Ecological Processes. Vol 3 of Encyclopedia of Ecology, 5 vols. Elsevier, Oxford. pp. 2511-2518.

Welsh D. 2000. Nitrogen fixation in seagrass meadows: Regulation , plant ± bacteria interactions and significance to primary productivity. Ecol. Lett. 3:58–71.

Yin G, Hou L, Liu M, Liu Z, Gardner WS. 2014. A novel membrane inlet mass spectrometer method to measure 15NH4+ for isotope-enrichment experiments in aquatic ecosystems. Environ. Sci. Technol. 48.

Tables and Figures

Table 1. Ambient nutrients ± SE (μM) and site conditions for sediment core incubation sites with (+M) and without (-M) macroalgae and non-incubation sites with (M1, M2) and without (NM1, NM2) macroalgae across St. Joseph Bay during June 2017. Depth (cm) is the distance from top of water column to sediment surface. BDL=below detection limit.

	Depth (cm)	Salinity	OP	NO_2^-	NO_3^-	NH_4^+	Urea
June 4th							
+M	75	35	0.35 ±0.00	0.39±0.03	0.67±0.07	0.93±0.04	0.47±0.10
-M	87	34	0.33 ±0.00	0.63±0.02	0.08±0.01	1.07±0.08	0.36±0.06
M1	52.5	34.5	0.21 ± 0.03	0.74±0.01	BDL	1.45±0.02	0.53±0.03
NM1	60.5	34.5	0.31 ±0.01	0.97±0.02	BDL	1.29±0.02	0.56±0.03
June 18th							
+M	78	31	0.28±0.02	0.47±0.02	BDL	1.73±0.12	0.60±0.01
-M	76	32	0.26±0.01	0.41±0.01	BDL	1.21±0.00	0.77±0.03
M1	68	32	0.27±0.01	0.66±0.02	BDL	1.26±0.04	0.56±0.01
M2	75	31	0.26±0.01	0.46±0.04	BDL	1.32±0.04	0.73±0.02
NM1	66	29	0.21±0.02	0.60±0.01	BDL	1.34±0.04	1.07±0.02
NM2	96	35	0.26±0.05	0.59±0.01	BDL	1.04±0.03	0.49±0.02
June 26th							
+M	109	32	0.25±0.00	0.70±0.03	BDL	1.20±0.00	0.74±0.04
-M	113	32	0.31±0.00	0.43±0.04	BDL	4.16±0.02	0.28±0.03
M1	83	29	0.24±0.01	0.44±0.01	BDL	1.02±0.03	0.18±0.01
M2	89	21	0.17±0.01	0.63±0.04	BDL	0.99±0.02	0.84±0.02
NM1	99	29	0.28±0.02	0.46±0.01	BDL	1.51±0.10	0.34±0.04
NM2	90	30	0.27±0.03	0.56±0.02	BDL	1.66±0.43	0.93±0.06

Table 2. Biomass measurements for *T.testudinum* (aboveground, belowground, shoot density) and macroalgae (g m^{-2}) ± SE, for sediment core incubation sites with (+M) and without (-M) macroalgae and non-incubation sites with (M1, M2) and without (NM1, NM2) macroalgae across St. Joseph Bay during June 2017. ND= no data

	Aboveground Biomass	Belowground Biomass	Macroalgae Biomass	Shoot Density	%Cover (*T.testudinum*)	%Cover (macroalgae)
June 4th						
+M	54.20	381.60	30.84	711.73	100	50.00±15.28
-M	193.81	730.34	ND	1642.45	98.33±1.67	ND
M1	139.06	851.34	10.95	930.72	100	40.00±14.43
NM1	319.18	1155.74	ND	1368.71	100	ND
June 18th						
+M	55.48±13.60	292.72±82.20	4.74±3.70	729.98±255.49	100	56.67±14.53
-M	146.36±21.30	745.85±46.11	ND	1970.94±109.50	90±5.77	ND
M1	78.84±8.28	374.11±75.13	29.38±12.13	656.98±83.63	100	36.67±17.64
M2	24.09±9.95	200.74±58.97	179.76±57.62	456.24±182.49	96.67±3.33	21.67±7.26
NM1	205.85±51.42	1168.15±297.97	ND	1715.45±203.22	100	20.00±15.28
NM2	52.74±12.49	401.31±105.15	ND	310.24±65.80	6.67±1.67	ND
June 26th						
+M	59.13±10.94	448.57±25.77	17.15±7.94	948.97±65.80	43.33±3.33	86.67±3.33
-M	190.52±38.16	735.82±37.78	ND	1770.20±363.62	70±15.28	ND
M1	121.72±33.37	404.77±41.66	4.93±1.92	656.98±54.75	100	13.33±6.01
M2	143.26±20.14	635.26±204.31	84.31±36.22	1478.20±383.24	86.67±6.67	20.00±11.55
NM1	230.31±11.11	1067.23±96.67	ND	2043.94±329.00	100	ND
NM2	107.49±30.65	901.52±320.52	ND	638.73±127.75	43.33±8.33	ND

Table 3. Sediment chemistry ± SE, for sediment core incubation sites with (+M) and without (-M) macroalgae and non-incubation sites with (M1, M2) and without (NM1, NM2) macroalgae across St. Joseph Bay during June 2017.

	Exchangeable NH_4^+ (µM)	Porewater NH_4^+ (µM)	Sulfide (µM)	% OM
June 4th				
+M	825.13 ± 128.42	491.67 ± 117.34	366.33 ± 1.99	3.60% ± 0.63%
-M	531.31 ± 29.66	369.09 ± 37.59	150.43 ± 53.78	1.60% ± 0.07%
M1	558.26 ± 40.95	400.77 ± 21.27	315.97 ± 26.99	3.69% ± 0.38%
NM1	581.13 ± 47.92	618.15 ± 119.05	63.40	5.39% ± 0.53%
June 18th				
+M	915.93 ± 102.82	506.45 ± 115.07	410.68 ± 2.93	3.47% ± 0.87%
-M	555.32 ± 72.59	312.90 ± 57.16	305.03 ± 51.07	2.02% ± 0.10%
M1	609.52 ± 65.49	432.29 ± 52.95	155.43 ± 72.09	4.10% ± 0.56%
M2	844.54 ± 243.89	874.73 ± 314.87	99.42 ± 81.04	1.72% ± 0.25%
NM1	613.27 ± 24.11	455.87 ± 68.95	96.63 ± 92.99	6.08% ± 1.05%
NM2	716.84 ± 62.04	789.75 ± 22.22	1.62 ± 1.62	1.02% ± 0.05%
June 26th				
+M	788.16 ± 39.48	342.20 ± 57.80	344.49 ± 71.20	4.14% ± 0.58%
-M	1161.36 ± 374.05	1006.72 ± 590.45	32.68 ± 17.14	2.31% ± 0.23%
M1	670.70 ± 129.88	464.91 ± 64.99	220.06 ± 53.77	3.18% ± 0.13%
M2	679.55 ± 61.92	605.26 ± 69.28	378.27 ± 27.78	2.63% ± 0.53%
NM1	496.70 ± 79.88	447.92 ± 102.67	213.55 ± 97.41	4.99% ± 0.12%
NM2	540.05 ± 123.42	716.01 ± 81.13	12.46 ± 2.71	0.49% ± 0.06%

Table 4. Sediment-water interface nutrient fluxes (μmole N or P m^{-2} hr^{-1}) ± standard error (SE) of duplicate cores from sites +M and -M. Samples collected for 3 days (n=6). Date refers to sediment core collection date. ND = no data.

	OP	NO_2^-	NO_3^-	NH_4^+	Urea	$^{28}N_2$	SOD
+M							
Control							
June 4th	-0.03 ± 0.47	-0.11 ± 1.27	-1.52 ± 0.02	-3.13 ± 5.23	-3.16±1.70	-18.76±28.16	2269.28±293.75
June 18th	-0.06 ± 0.57	-0.76 ± 1.79	-0.46 ± 0.24	31.90 ± 16.14	-3.00±1.99	-79.90±12.08	2856.87±288.52
June 26th	0.01 ± 0.12	-4.24 ± 3.78	4.21 ± 4.00	30.20 ± 18.09	0.75±2.03	-8.43±7.76	2128.06±313.98
$^{15}NH_4^+$							
June 4th	0.93±1.25	1.28±1.85	0.33±0.59	-104.69±21.55	-10.07±9.27	-147.49±26.63	2918.34±226.08
June 18th	1.15±0.59	-0.72±0.58	-0.29±0.71	25.73±24.61	1.02±2.13	-94.41±22.37	3097.93±259.94
June 26th	-0.35±0.30	0.41±1.35	0.50±0.70	8.45±22.76	3.41±2.79	-3.65±7.35	2307.09±214.97
$^{15}NO_3^-$							
June 4th	-0.09±1.23	49.50±3.819	-291.35±41.37	51.04±13.41	1.54±0.96	-30.52±14.73	2747.53±221.42
June 18th	-1.01±0.91	44.01±7.58	-288.19±100.68	50.33±12.02	-1.21±1.92	-1.34±13.65	2560.64±115.54
June 26th	-0.14±0.14	67.75±5.14	-218.28±68.45	147.95±22.50	1.66±0.57	1.97±20.64	2405.04±459.66
-M							
Control							
June 4th	-0.16 ± 0.16	1.74 ± 1.40	-0.92 ± 0.30	8.71 ± 1.73	3.16±4.73	-47.64±12.71	1539.88±405.84
June 18th	-5.57 ± 5.07	-0.76 ± 0.68	-0.84 ± 0.89	48.48 ± 24.12	5.17±0.16	-76.56±23.93	2314.18±300.73
June 26th	0.08 ± 0.11	0.82 ± 1.30	1.08 ± 0.49	71.89 ± 53.43	-0.81±1.79	-16.79±4.71	1188.98±130.75
$^{15}NH_4^+$							
June 4th	0.00±0.24	-0.26±1.114	-0.24±0.90	36.53±26.18	1.61±2.58	-34.59±13.56	1644.53±108.51
June 18th	-4.26±2.94	-0.61±1.61	-0.82±1.60	89.12±7.10	0.18±1.70	-17.53±4.17	1813.61±156.13
June 26th	0.10±0.45	-0.23±0.94	5.67±4.77	20.56±5.95	0.49±1.93	20.04±10.22	1444.78±175.72
$^{15}NO_3^-$							
June 4th	-0.15±0.13	23.64±9.456	-215.02±34.47	123.05±38.03	6.08±4.50	9.49±14.61	1385.95±246.72
June 18th	-0.14±0.16	32.12±5.97	-228.96±61.82	155.15±23.10	1.03±1.69	-6.08±13.76	1411.62±76.50
June 26th	0.29±0.32	68.71±23.09	-231.13±18.79	143.21±65.80	1.17±0.51	-21.07±6.54	1401.18±145.57

Table 5. Spearman correlation coefficients for biogeochemical data from all dates and sites. Number in parenthesis is n for comparisons.

Factor	EX NH_4^+	% Cover (macro.)	% Cover (seagrass)	Shoot density	% OM	PW NH_4^+	Sulfide	Algae Biomass	Below. Biomass	Above Biomass
Above Biomass	-0.401*(40)	-0.439** (40)	0.227 (40)	0.762** (40)	0.327* (39)	-0.148 (40)	0.034 (38)	-0.486**(40)	0.797** (40)	-
Below Biomass	-0.366* (40)	-0.408** (40)	0.099 (40)	0.736** (40)	0.228 (39)	-0.065 (40)	0.055 (38)	-0.531** (40)	-	
Algae Biomass	0.234 (48)	0.573** (48)	0.102 (48)	-0.347* (40)	0.069 (47)	-0.40 (48)	0.289 (45)	-		
Sulfide	0.205 (45)	0.511** (45)	0.364* (45)	0.385* (38)	0.418** (44)	-0.267 (45)	-			
PW NH_4^+	0.441** (48)	-0.171 (48)	-0.207 (48)	-0.264 (40)	-0.274 (47)	-				
% OM	-0.059 (47)	0.317* (47)	0.523** (47)	0.310 (39)	-					
Shoot density	-0.15 1(40)	-0.267 (40)	-0.201 (40)	-						
% Cover (seagrass)	-0.182 (48)	0.190 (48)	-							
% Cover (macro)	0.257 (48)	-								
EX NH_4^+	-									

* indicates significance at $\alpha = 0.05$.

** indicates significance at $\alpha = 0.01$.

Table 6. Spearman correlation coefficients for unamended cores with no macroalgae, all comparisons were made with n=18.

Factor	SOD	$^{28}N_2$	NH_4^+	OP	NO_2^-	NO_3^-	Urea
Urea	0.649**	-0.228	0.1189	-0.212	0.015	-0.428	-
NO_3^-	-0.325	0.009	0.172	-0.001	-0.366	-	
NO_2^-	0.069	0.046	-0.053	0.024	-		
OP	-0.026	0.366	-0.321	-			
NH_4^+	0.007	-0.238	-				
$^{28}N_2$	-0.624**	-					
SOD	-						

** indicates significance at $\alpha = 0.01$.

Table 7. Spearman correlation coefficients for unamended cores with macroalgae, all comparisons were made with n=18.

Factor	SOD	$^{28}N_2$	NH_4^+	OP	NO_2^-	NO_3^-	Urea
Urea	-0.331	0.313	0.238	0.218	-0.119	0.214	-
NO_3^-	0.057	0.300	0.571*	-0.325	-0.247	-	
NO_2^-	-0.049	-0.257	-0.168	-0.261	-		
OP	-0.216	0.366	0.057	-			
NH_4^+	0.463	0.587	-				
$^{28}N_2$	-0.554*	-					
SOD	-						

* indicates significance at $\alpha = 0.05$.

Table 8. Spearman correlation coefficients for $^{15}NH_4^+$ addition cores with no macroalgae, all comparisons were made with n=18.

Factor	SOD	$^{28}N_2$	$^{29}N_2$	NH_4^+	OP	NO_2^-	NO_3^-	Urea
Urea	0.069	-0.337	-0.267	-0.053	0.544*	-0.240	-0.203	-
NO_3^-	-0.102	0.139	0.127	-0.527*	-0.046	-0.459	-	
NO_2^-	0.005	-0.112	-0.061	0.214	0.152	-		
OP	-0.280	0.240	-0.713**	-0.377	-			
NH_4^+	0.214	-0.379	0.430	-				
$^{29}N_2$	0.571*	-0.476	-					
$^{28}N_2$	-0.278	-						
SOD	-							

* indicates significance at $\alpha = 0.05$.

** indicates significance at $\alpha = 0.01$.

Table 9. Spearman correlation coefficients for $^{15}NH_4^+$ addition cores with macroalgae, all comparisons were made with n=18.

Factor	SOD	$^{28}N_2$	$^{29}N_2$	NH_4^+	OP	NO_2^-	NO_3^-	Urea
Urea	-0.370	0.424	0.317	0.560*	0.170	0.158	-0.410	-
NO_3^-	-0.226	0.026	-0.189	-0.112	-0.410	-0.467	-	
NO_2^-	-0.160	-0.003	-0.032	-0.022	0.441	-		
OP	0.333	-0.385	0.556*	0.079	-			
NH_4^+	-0.311	0.610**	-0.110	-				
$^{29}N_2$	0.311	-0.550*	-					
$^{28}N_2$	-0.707**	-						
SOD	-							

* indicates significance at $\alpha = 0.05$.

** indicates significance at $\alpha = 0.01$.

Table 10. Spearman correlations for $^{15}NO_3^-$ addition cores with no macroalgae, n=18 for all comparisons

Factor	SOD	$^{28}N_2$	$^{29}N_2$	$^{30}N_2$	Pot. DNF	Pot. DNRA	N-fix	NH_4^+	OP	NO_2^-	NO_3^-	Urea
Urea	0.164	-0.030	-0.034	0.079	0.042	0.007	0.030	0.049	0.015	0.034	-0.082	-
NO_3^-	-0.036	0.044	-0.028	-0.092	0.129	-0.109	-0.044	-0.513*	-0.335	-0.358	-	
NO_2^-	0.628**	-0.317	0.061	0.348	-0.141	0.527*	0.317	0.814**	0.476*	-		
OP	0.399	-0.335	0.009	0.480*	0.141	0.691*	0.335	0.531*	-			
NH_4^+	0.612**	-0.197	0.228	0.484*	-0.022	0.512*	0.197	-				
N-Fix	0.383	-1.000**	0.245	0.412	-0.416	0.239	-					
Pot. DNRA	0.727**	-0.239	0.454	0.668**	0.477*	-						
Pot. DNF	0.346	0.416	0.439	0.401	-							
$^{30}N_2$	0.754**	-0.412	0.591**	-								
$^{29}N_2$	0.598**	-0.245	-									
$^{28}N_2$	-0.383	-										
SOD	-											

* indicates significance at $\alpha = 0.05$.

** indicates significance at $\alpha = 0.01$.

Table 11. Spearman correlations for all $^{15}NO_3^-$ addition cores with macroalgae, n=18 for all comparisons

Factor	SOD	$^{28}N_2$	$^{29}N_2$	$^{30}N_2$	Pot. DNF	Pot. DNRA	N-fix	NH_4^+	OP	NO_2^-	NO_3^-	Urea
Urea	0.125	-0.253	0.344	-0.032	0.065	0.337	0.253	0.193	0.038	0.011	-0.059	-
NO_3^-	-0.616**	-0.125	-0.414	-0.548*	-0.203	-0.126	0.125	-0.273	-0.496*	-0.259	-	
NO_2^-	0.482*	-0.558*	0.356	0.263	-0.286	0.595**	0.558*	0.430	0.172	-		
OP	0.133	0.096	0.313	0.222	0.106	-0.135	-0.096	-0.094	-			
NH_4^+	0.560*	-0.298	0.094	0.123	0.013	0.234	0.298	-				
N-Fix	0.253	-1.000**	0.562*	-0.135	-0.666**	0.438	-					
Pot. DNRA	0.194	-0.438	0.243	0.421	-0.090	-						
Pot. DNF	-0.063	-0.666**	-0.073	0.366	-							
$^{30}N_2$	0.230	0.135	0.185	-								
$^{29}N_2$	0.364	-0.562*	-									
$^{28}N_2$	-0.253	-										
SOD	-											

* indicates significance at $\alpha = 0.05$.

** indicates significance at $\alpha = 0.01$.

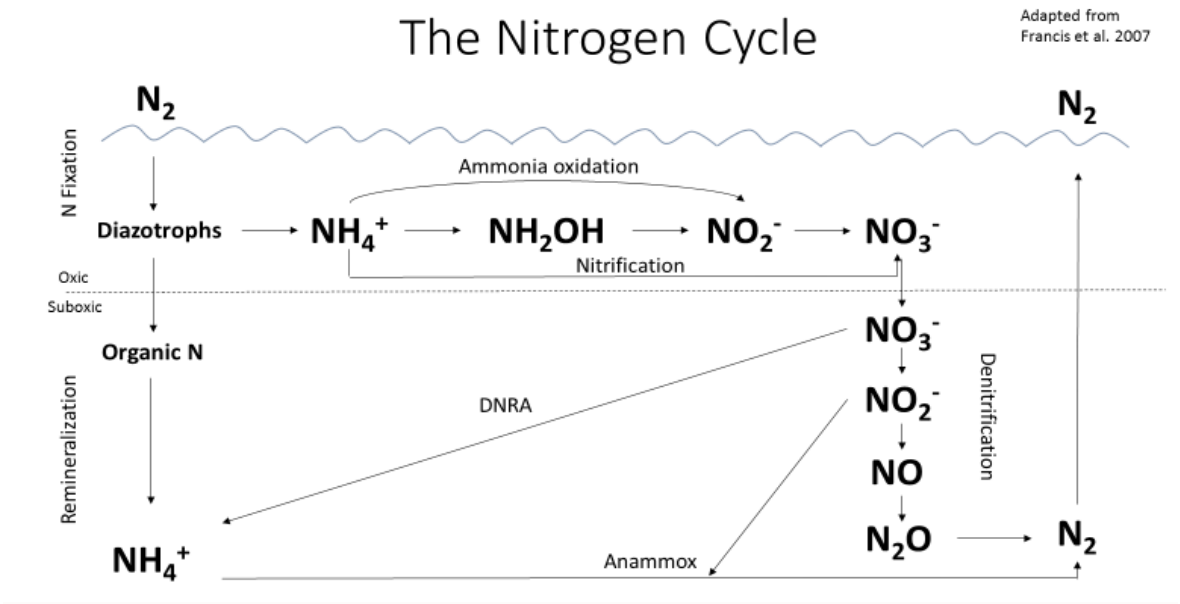

Figure 1. Sediment nitrogen cycling diagram, adapted from Francis et al. 2007.

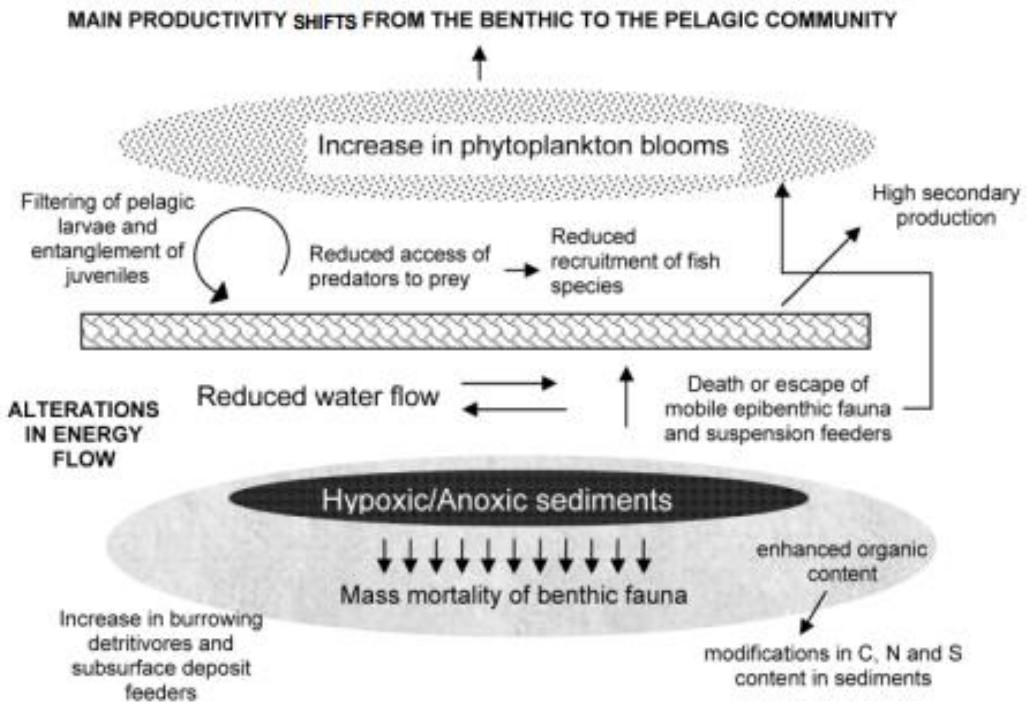

Figure 2. Common effects of drift macroalgae on soft benthic sediments (Arroyo and Bonsdorff 2016).

Figure 3. Map of St. Joseph Bay, FL, in the northern Gulf of Mexico (Google Earth). GPS site locations: NM1: N29°42.317' W085°198.432', NM2: N29°51.335' W085°23.885', M1: N29°43.078' W085°20.237', M2: N29°46.661' W085°23.913', +M: N29°43.078' W085°20.237', -M: N29°41.611' W085°21.709'

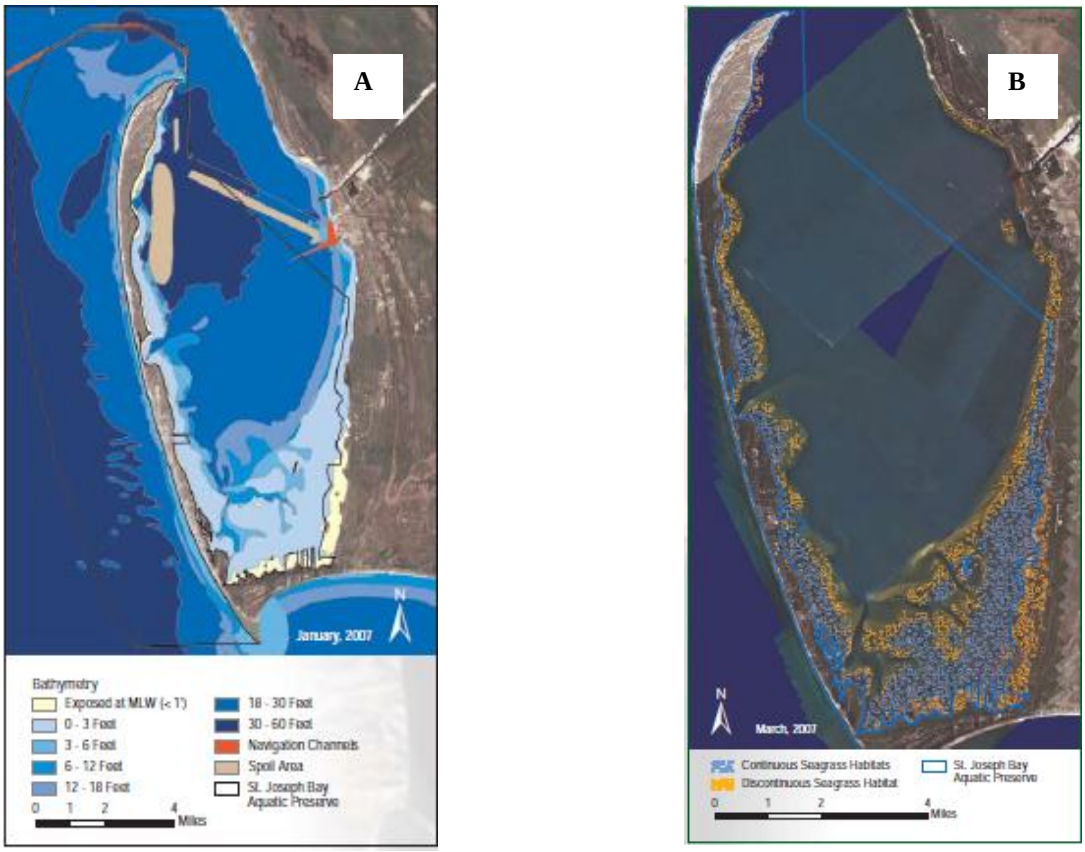

Figure 4. Panel A is a bathymetry map, while panel B is a map of seagrass cover in St. Joseph Bay, FL (FDEP 2008).

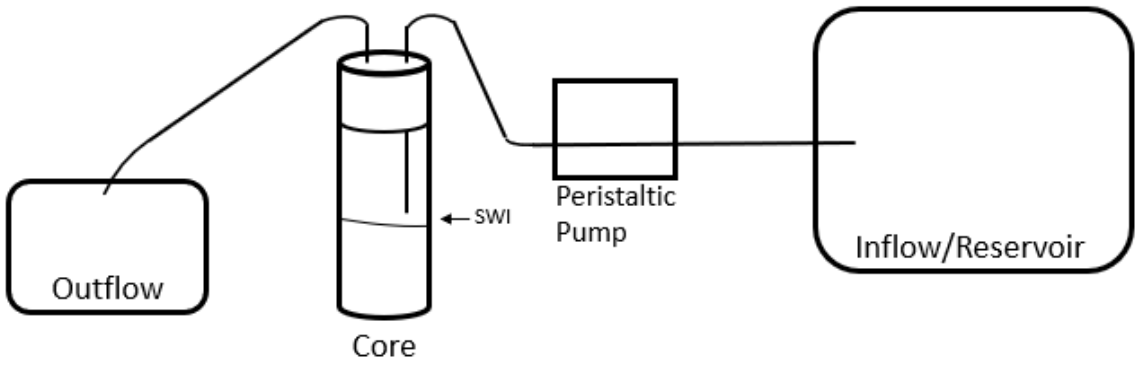

Figure 5. Diagram of continuous-flow incubation system. SWI is the sediment water interface.

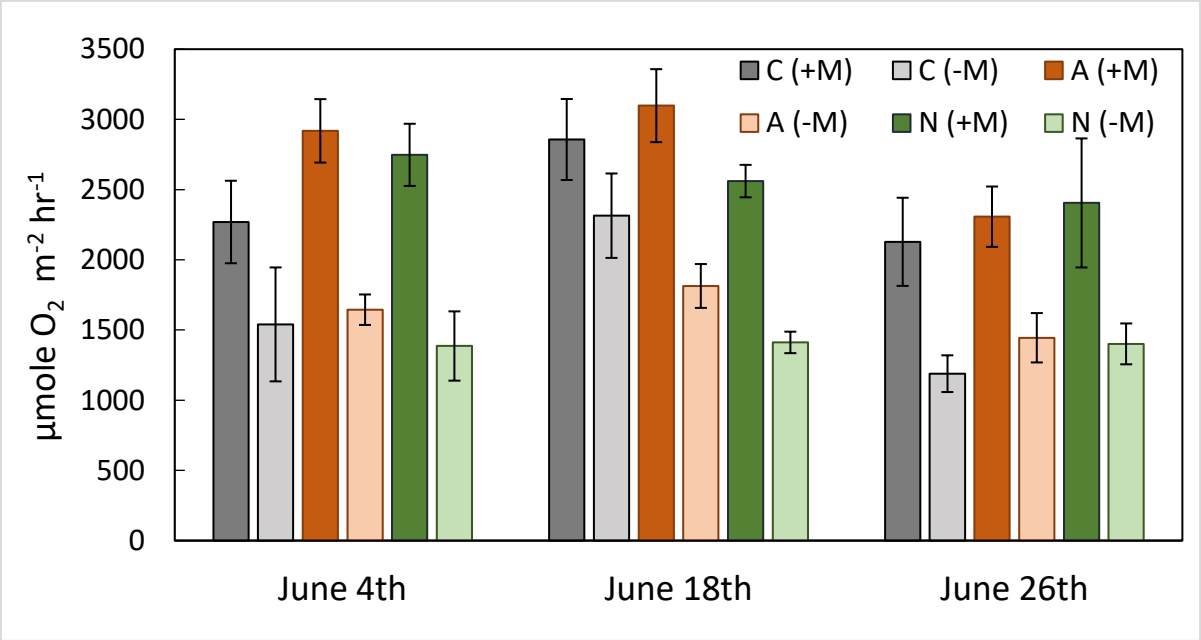

Figure 6. Sediment oxygen demand (SOD) averages (n=6) for all cores.

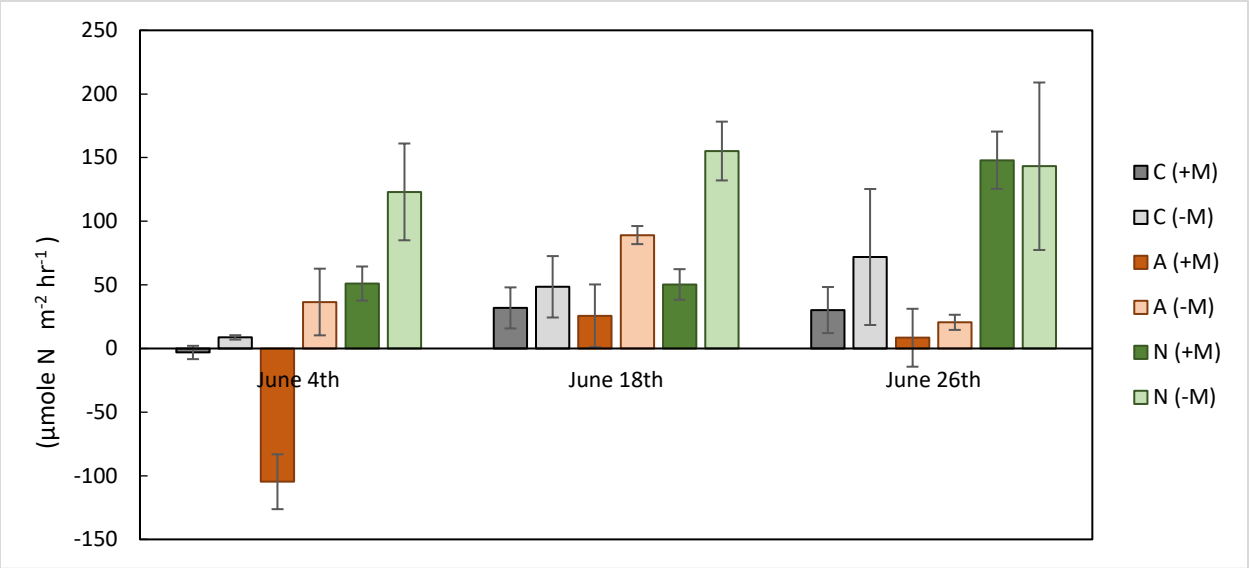

Figure 7. NH_4^+ fluxes.

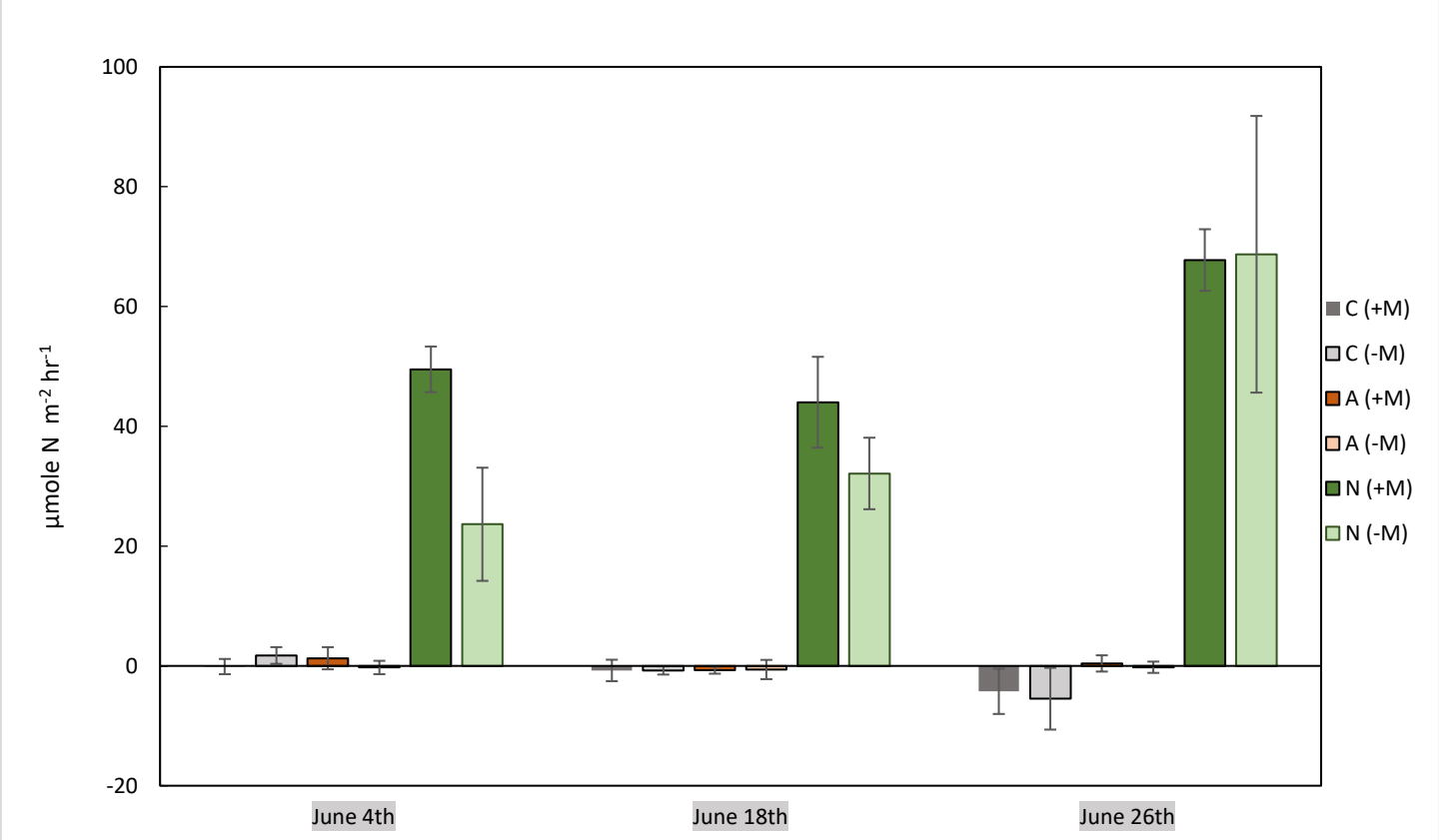

Figure 8. NO_2^- fluxes**.**

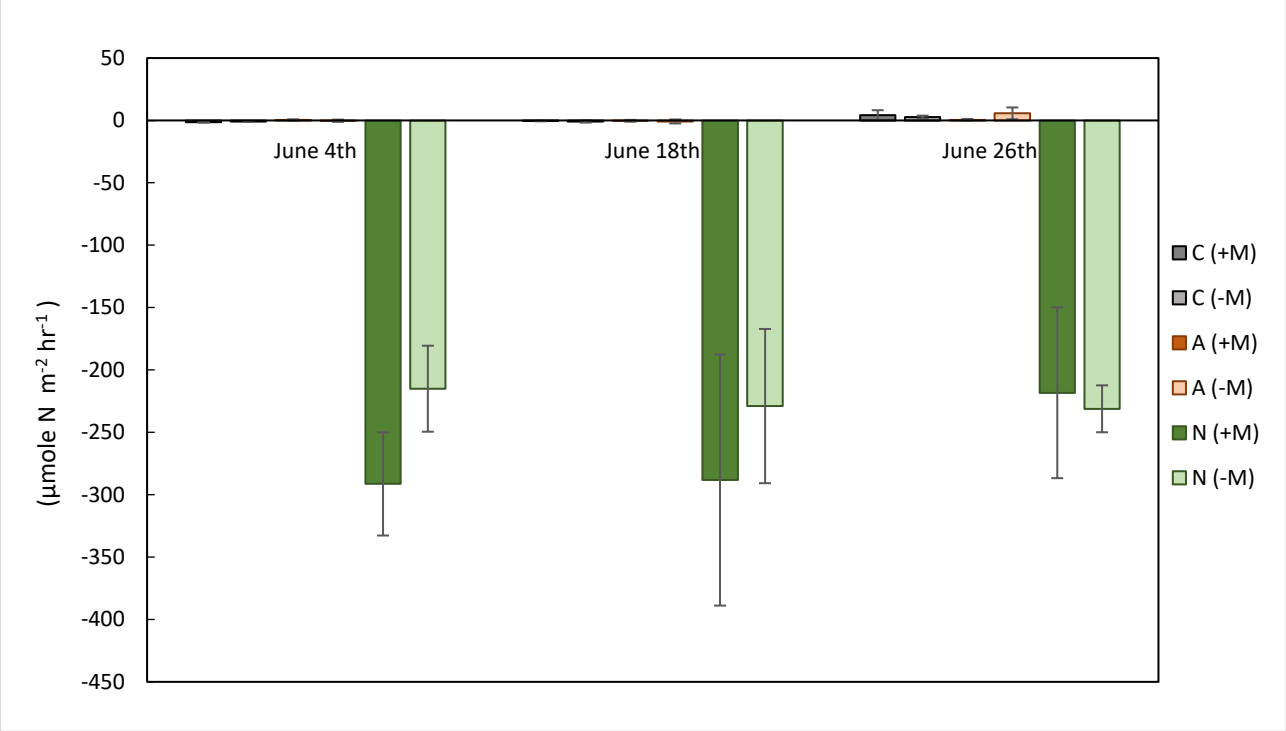

Figure 9. NO_3^- fluxes.

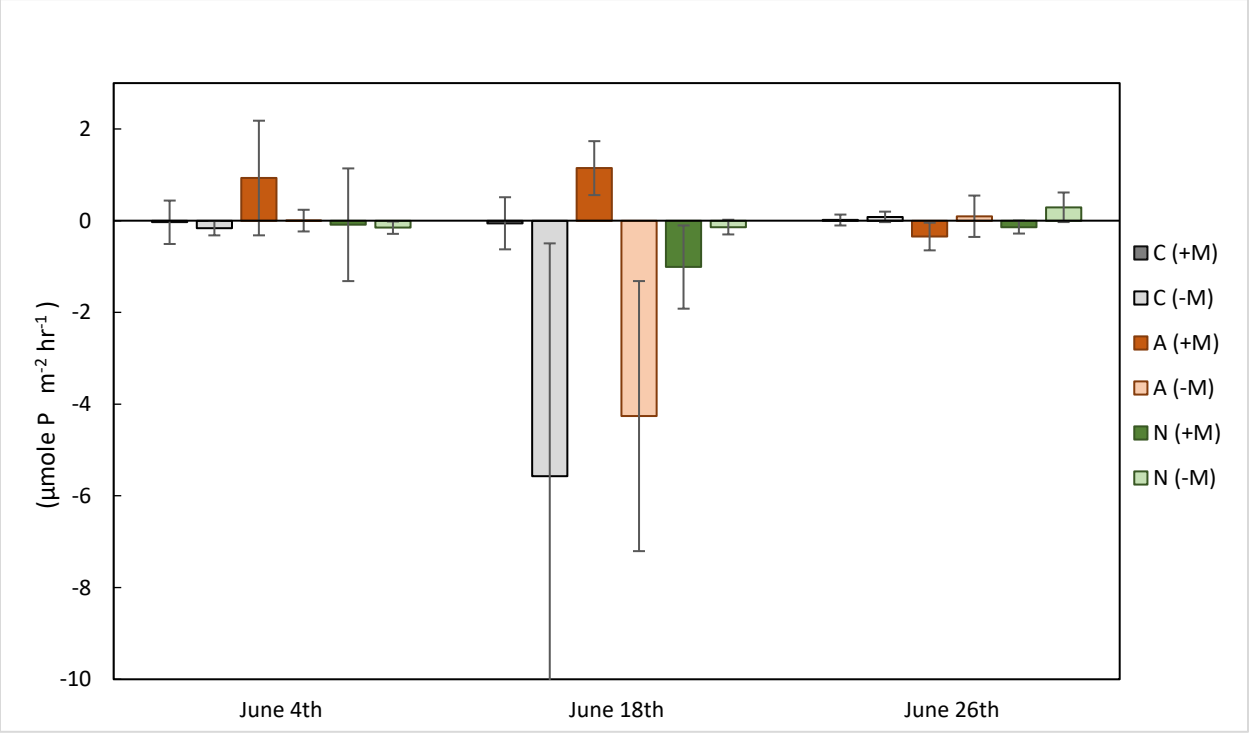

Figure 10. OP fluxes.

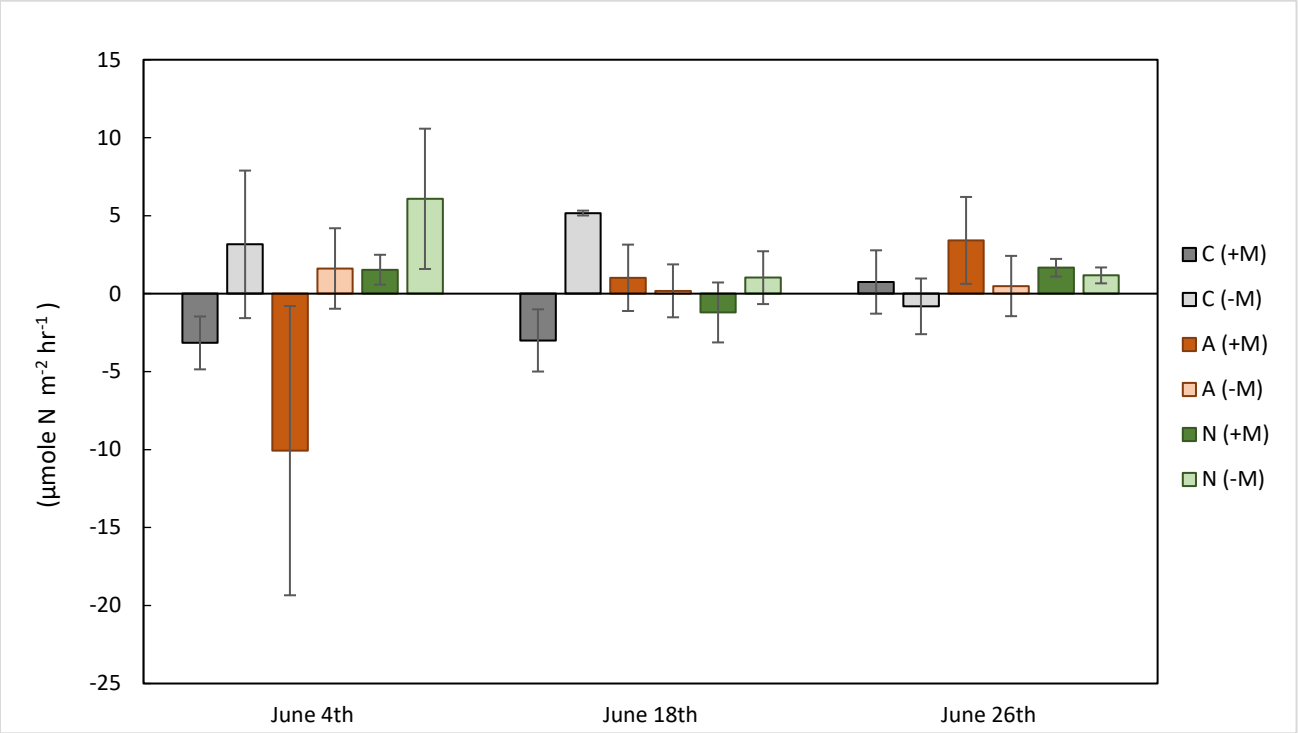

Figure 11. Urea fluxes.

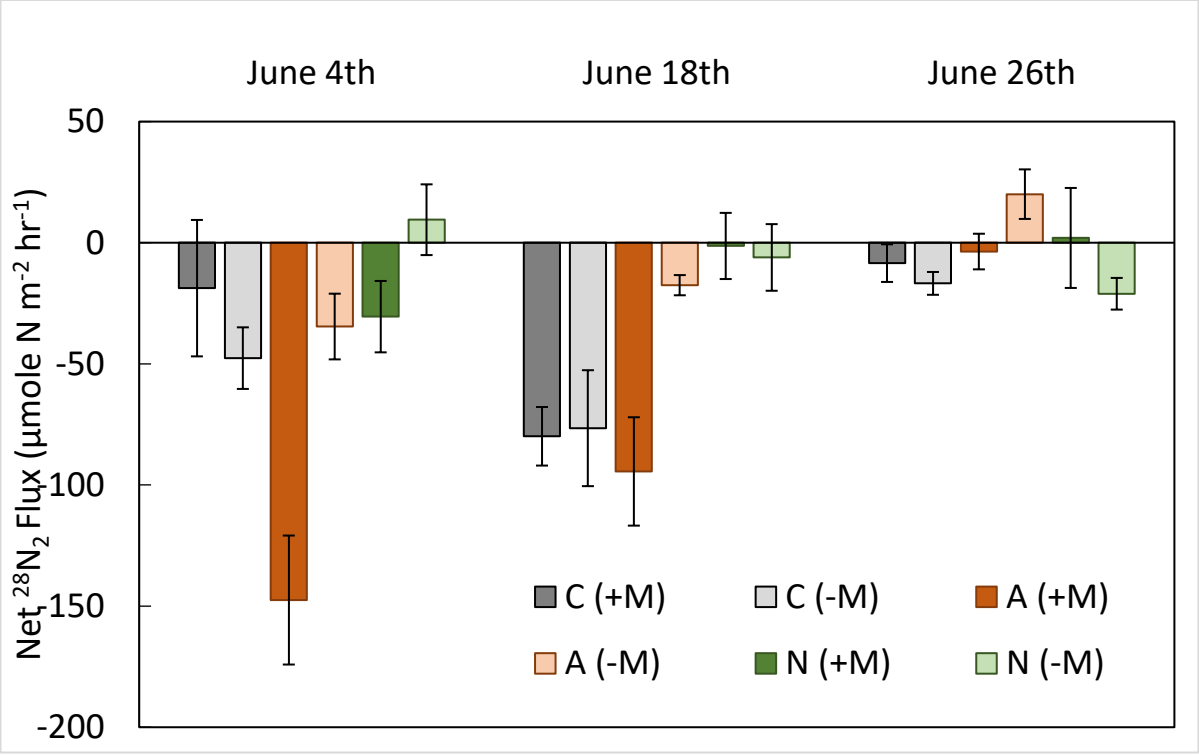

Figure 12. Net 28N2 Fluxes.

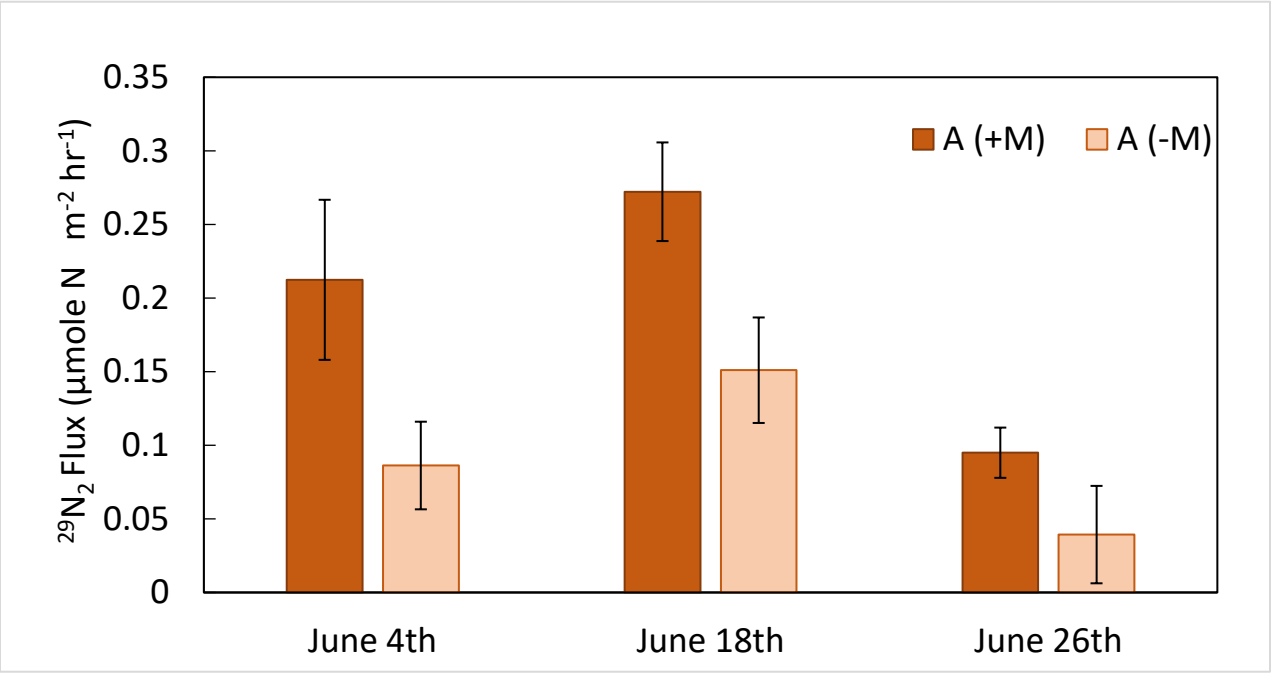

Figure 13. Possible anammox, $^{29}N_2$ production in $^{15}NH_4^+$ cores.

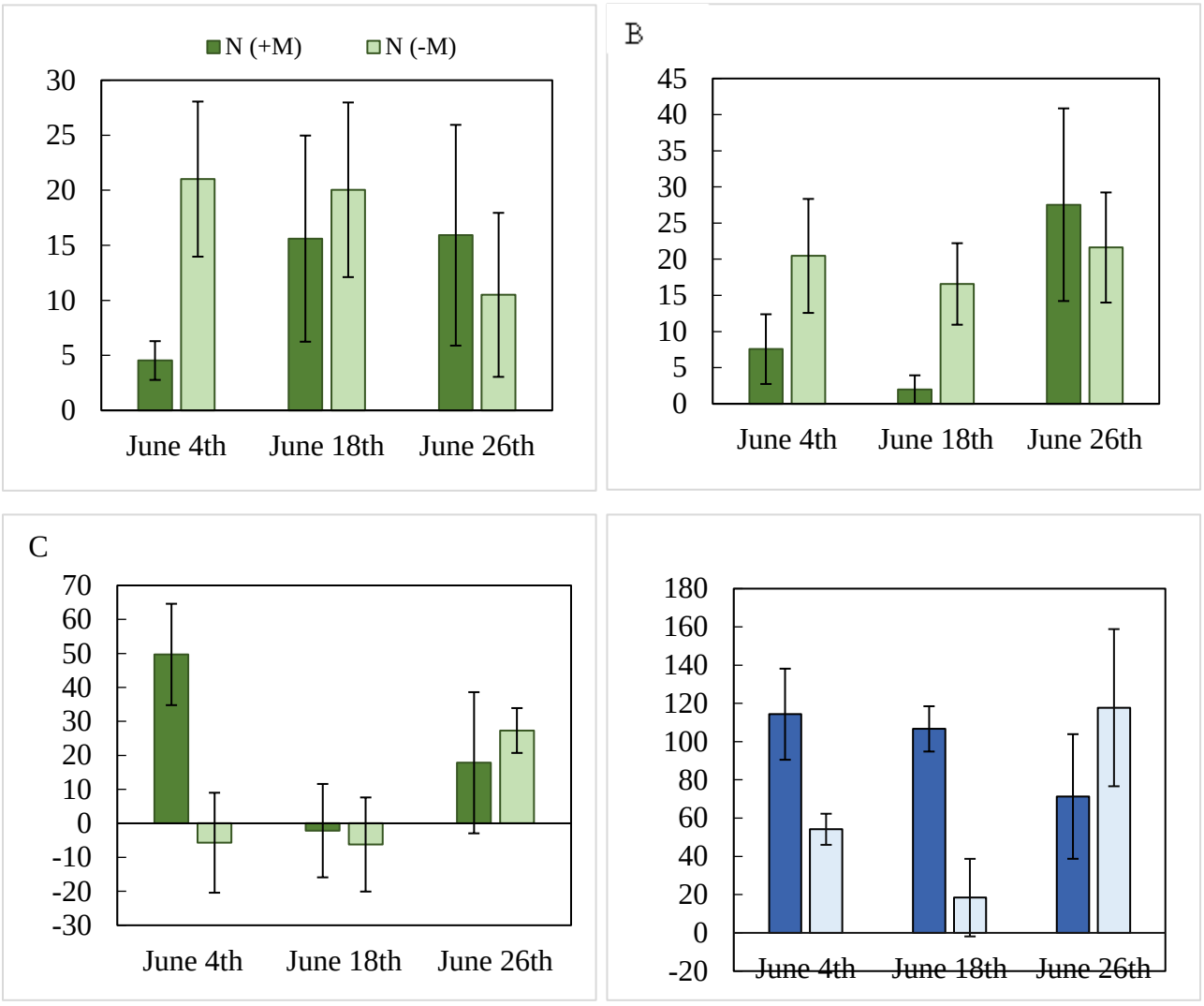

Figure 14. Panel A is potential DNF, panel B is potential DNRA, panel C is calculated N-fixation, and panel D is NIAF, all measured in µmole N m^{-2} hr^{-1}. All green bars represent measurements from $^{15}NO_3^-$ addition cores, while NIAF bars are in blue because they are the difference in $^{15}NH_4^+$ concentration between unamended and $^{15}NO_3^-$ addition cores.